AEDC-TR-85-39

Method to Detect Ethylene Glycol in Gaseous Mixtures

R. E. Willis
Mercer University
Consultant, Sverdrup Technology, Inc.

August 1985

Final Report For Period October 1, 1982 – September 30, 1983

ARNOLD ENGINEERING DEVELOPMENT CENTER
ARNOLD AIR FORCE STATION, TENNESSEE
AIR FORCE SYSTEMS COMMAND
UNITED STATES AIR FORCE

NOTICES

When U. S. Government drawings, specifications, or other data are used for any purpose other than a definitely related Government procurement operation, the Government thereby incurs no responsibility nor any obligation whatsoever, and the fact that the government may have formulated, furnished, or in any way supplied the said drawings, specifications, or other data, is not to be regarded by implication or otherwise, or in any manner licensing the holder or any other person or corporation, or conveying any rights or permission to manufacture, use, or sell any patented invention that may in any way be related thereto.

Qualified users may obtain copies of this report from the Defense Technical Information Center.

References to named commercial products in this report are not to be considered in any sense as an endorsement of the product by the United States Air Force or the Government.

This report has been reviewed by the Office of Public Affairs (PA) and is releasable to the National Technical Information Service (NTIS). At NTIS, it will be available to the general public, including foreign nations.

APPROVAL STATEMENT

This report has been reviewed and approved.

Frank T. Tanji

FRANK T. TANJI, Captain, USAF
Directorate of Technology
Deputy for Operations

Approved for publication:

FOR THE COMMANDER

Marion L. Laster

MARION L. LASTER
Director of Technology
Deputy for Operations

UNCLASSIFIED

SECURITY CLASSIFICATION OF THIS PAGE

REPORT DOCUMENTATION PAGE

1a REPORT SECURITY CLASSIFICATION UNCLASSIFIED	1b RESTRICTIVE MARKINGS
2a SECURITY CLASSIFICATION AUTHORITY	3 DISTRIBUTION/AVAILABILITY OF REPORT See Reverse of This Page.
2b DECLASSIFICATION/DOWNGRADING SCHEDULE	
4 PERFORMING ORGANIZATION REPORT NUMBER(S) AEDC-TR-85-39	5 MONITORING ORGANIZATION REPORT NUMBER(S)
6a NAME OF PERFORMING ORGANIZATION Arnold Engineering Development Center 6b. OFFICE SYMBOL (If applicable) DOT	7a. NAME OF MONITORING ORGANIZATION
6c ADDRESS (City, State and ZIP Code) Air Force Systems Command Arnold Air Force Station, TN 37389-5000	7b ADDRESS (City, State and ZIP Code)
8a. NAME OF FUNDING/SPONSORING ORGANIZATION Arnold Engineering Development Center 8b. OFFICE SYMBOL (If applicable) DO	9 PROCUREMENT INSTRUMENT IDENTIFICATION NUMBER
8c. ADDRESS (City, State and ZIP Code) Air Force Systems Command Arnold Air Force Station, TN 37389-5000	10 SOURCE OF FUNDING NOS PROGRAM ELEMENT NO: 65807F PROJECT NO TASK NO WORK UNIT NO
11 TITLE (Include Security Classification) See Reverse of This Page.	
12. PERSONAL AUTHOR(S) Willis, R. E., Mercer University, Consultant, Sverdrup Technology, Inc., AEDC Group	
13a. TYPE OF REPORT Final Report 13b. TIME COVERED FROM 10/1/82 TO 9/30/83	14 DATE OF REPORT (Yr., Mo., Day) August 1985 15 PAGE COUNT 55
16. SUPPLEMENTARY NOTATION Available in Defense Technical Information Center (DTIC).	

17 COSATI CODES			18 SUBJECT TERMS (Continue on reverse if necessary and identify by block number)	
FIELD	GROUP	SUB GR		
07	04		ethylene glycol	monitor
			microwave spectroscopy	microwave spectrometer
20	06		spectra	(Cont)

19. ABSTRACT (Continue on reverse if necessary and identify by block number)

A study was conducted to determine if microwave spectroscopy techniques could be used to monitor the level of ethylene glycol in the inlet airstream to the Engine Test Facility (ETF) test cells during simulated altitude testing. The theory of microwave spectroscopy and the spectra of ethylene glycol are reviewed. Three separate designs of microwave spectrometers are presented which should be capable of monitoring ethylene glycol in the inlet airstreams with a sensitivity of at least 10 ppm.

20 DISTRIBUTION/AVAILABILITY OF ABSTRACT UNCLASSIFIED/UNLIMITED ☐ SAME AS RPT ☒ DTIC USERS ☐	21 ABSTRACT SECURITY CLASSIFICATION UNCLASSIFIED
22a. NAME OF RESPONSIBLE INDIVIDUAL W. O. Cole	22b TELEPHONE NUMBER (Include Area Code) (615) 454-7813 22c OFFICE SYMBOL DOS

DD FORM 1473, 83 APR EDITION OF 1 JAN 73 IS OBSOLETE

UNCLASSIFIED

SECURITY CLASSIFICATION OF THIS PAGE

3. DISTRIBUTION/AVAILABILITY OF REPORT

Approved for public release; distribution unlimited.

11. TITLE

Method to Detect Ethylene Glycol in Gaseous Mixtures

18. SUBJECT TERMS (Continued)

line width
half-width
pressure broadening

PREFACE

The work reported herein was conducted by the Arnold Engineering Development Center (AEDC), Air Force Systems Command (AFSC), Arnold Air Force Station, Tennessee 37389-5000. The results were obtained by Sverdrup Technology, Inc. (STI), AEDC Group, operating contractor for the propulsion test facility at AEDC under Project Number D239. The work was performed by Dr. R. E. Willis of Mercer University under STI subcontract No. A83-ED-018. The Air Force Program Manager was Capt. F. T. Tanji. The Sverdrup Project Manager was H. C. Walker, Jr. The research was performed from October 1, 1982 to September 30, 1983, and the manuscript was submitted for publication on March 4, 1985.

CONTENTS

Page

1.0 INTRODUCTION 5
2.0 THEORY 6
2.1 Rotational Energies and Transition Frequencies 6
2.2 Symmetric-Top Molecules 10
2.3 Asymmetric-Top Molecules 14
2.4 Effect of an Applied Electric Field and Stark Modulation Spectrometers 16
2.5 Line Strengths 17
3.0 SPECTRA OF ETHYLENE GLYCOL 21
4.0 DETECTION OF ETHYLENE GLYCOL 23
4.1 Fast-Scan, Low-Resolution Spectrometer 24
4.2 Simple Spectrometer to Detect Ethylene Glycol 28
4.3 Calibration 30
4.4 Resonant-Cavity Spectrometer 32
5.0 CONCLUSION 38
REFERENCES 39

ILLUSTRATIONS

Figure Page

1. Hyperfine Structure of ^{79}BrF $J = 9 \rightarrow 10$, $v = 2$ 5
2. Most Likely Conformer of Ethylene Glycol 22
3. Terminated Waveguide 24
4. Details of Stark Cell Construction 26
5. Diagram of Stark Modulation Spectrometer 27
6. Simple Spectrometer for Which a Gunn Effect Diode Is Both Oscillator and Detector 29
7. Calibration Manifold 31
8. Semiconfocal Resonant Cavity 33
9. Resonant-Cavity Spectrometer 35

APPENDIXES

A. Microwave Spectrum of Ethylene Glycol 41
B. Vibrational Frequencies of Ethylene Glycol 48
C. Parts Lists for Proposed Spectrometer Designs 49
D. Compact 10-kHz Stark Modulator 51

1.0 INTRODUCTION

The work reported herein consisted of a study of whether the techniques of microwave spectroscopy would be used to identify small concentrations of ethylene glycol in the airstreams. A particular application is to the inlet air supplied to jet engines during simulated altitude testing.

Ethylene glycol is used as a refrigerant for the intake air during simulated altitude testing. There have been some problems during these tests because of the ethylene glycol accidentally leaking into the inlet airstream. Since ethylene glycol has at times been suspected of interfering with the test article, its early detection would be greatly beneficial so that testing could be stopped before damage occurs. Because a detection scheme must indicate the presence of ethylene glycol as soon as it appears in the inlet airstream, a spectroscopic technique is preferred over other methods of gas analysis such as sampling and subsequent laboratory analysis.

The standard chemical technique of infrared spectroscopy would be difficult to apply in this case because of the complex structure of the molecule; i.e., the infrared frequency vibrational bands would be so diffuse that absorption at a particular frequency would be very small. The requirement of immediate detection would not allow time for a sufficient concentration of a sample to be collected.

The technique of microwave spectroscopy detection of pure, rotational lines is characterized by extremely high resolution, sensitivity, and specificity. In microwave spectroscopy, resolution is defined as the peak absorption frequency divided by the full width of the line at the half-maximum intensity. Typically, resolution is of the order of approximately 50,000 and with additional care, even 500,000. The absorption lines observed in this frequency region are between rotational energy levels of the same vibrational state, usually the ground vibrational state. An example of the resolution obtainable is shown in Fig. 1 for the J = 9 – 10, v = 2 transition at 209.4 GHz of the ^{79}BrF molecule.

Figure 1. Hyperfine structure of ^{79}BrF, J = 9 – 10, v = 2.

To obtain high resolution, the pressure in the absorption cell must be kept low; the lower the pressure, the higher the resolution. For the above spectrum, the pressure was on the order of 1 mtorr. Greater sample pressure would be needed in order to have sufficient concentration of the absorbing molecule in a dilute mixture, but the resolution would still be sufficient to uniquely determine the presence of ethylene glycol.

The theory of absorption coefficients and the minimum concentration of ethylene glycol that could be detected will be discussed in detail later in this report. In summary, it should be possible to detect a concentration as low as 10 ppm with an inexpensive "bare bones" spectrometer. With greater sophistication, even higher sensitivity can be obtained.

High-resolution microwave spectroscopy offers a unique approach for the unambiguous identification and characterization of a gaseous component in a mixture, provided that the rotational absorption spectrum can be observed experimentally. A molecule must possess a permanent electric dipole moment if its rotational absorption spectrum is to be observed at all in the vapor state. A microwave spectral pattern that is unique both as to frequencies and relative intensities is associated with any polar molecular species. In other words, two different molecules or even any two isotopic species of the same molecule (e.g., ^{79}BrF and ^{81}BrF) have considerably different rotational spectra.

Since the usefulness of the technique will be enhanced by an understanding of some of the basic theory, the first section of this report will outline some of the fundamental elements of the theory of rotational transitions using the texts cited as Refs. 1 and 2. The second part of the report will detail what is known about the spectrum of ethylene glycol. The final section will present a discussion of specific spectroscopic techniques and spectrometer designs appropriate to the rapid identification of ethylene glycol in airstreams.

2.0 THEORY

2.1 ROTATIONAL ENERGIES AND TRANSITION FREQUENCIES

To describe the gross features of the microwave spectrum of most molecules, it is sufficient to regard a molecule as consisting of point masses with fixed interatomic distances. This model of a rigid rotor serves to point out many of the advantages, unique capabilities, and disadvantages inherent in microwave spectroscopy. Derivation of the quantum mechanical properties of molecular rotors, including their microwave spectra, begins with the classical expressions for the angular momenta and rotational energy. Hence, we begin with a brief summary of the classical mechanics of rotating bodies.

The classical angular momentum of a rigid system of particles is

$$\overline{P} = \overline{\overline{I}} \times \overline{\omega} \tag{1}$$

where ω is the angular velocity and I is the moment of inertia tensor. The origin of the coordinate system is chosen at the center of mass since this choice allows the total kinetic energy to be written as the sum of the kinetic energy of translational motion of the center of mass plus the kinetic energy of the motion relative to the center of mass. The translational and rotational motions can hence be treated separately. It is always possible to choose the coordinate axes in such a way that the products of inertia vanish, leaving only the diagonal elements, called the principal moments of inertia. These depend on the masses m_i of the nuclei and their coordinates ($x_i = y_i$, and z_i) in the principal inertial axis system of the molecule

$$I_{xx} = \Sigma\, m_i(y_i^2 + z_i^2) \tag{2}$$

where I_{xx} is the moment of inertia about the x axis and permutation of x, y, and z yield expressions for I_{yy} and I_{zz}. In the principal axis system, the components of angular momentum become

$$P_x = I_x\omega_x,\ P_y = I_y\omega_y,\ P_z = I_z\omega_z \tag{3}$$

The rotational kinetic energy in the principal axis system is given by

$$E_r = \tfrac{1}{2}I_x\omega_x^2 + \tfrac{1}{2}I_y\omega_y^2 + \tfrac{1}{2}I_z\omega_z^2 = \tfrac{1}{2}\left[\left(\frac{P_x^2}{I_x}\right) + \left(\frac{P_y^2}{I_y}\right) + \left(\frac{P_z^2}{I_z}\right)\right] \tag{4}$$

As indicated above x, y, and z refer to the principal axes' coordinate system fixed in the body. X, Y, and Z will refer to a coordinate system whose origin is the center of mass, but whose directions are fixed in space. The time rate of change of angular momentum relative to the space-fixed axes is equal to the applied torque. In the absence of externally applied torques, $dP/dt = 0$, it is evident that

$$\overline{P} = iP_X + jP_Y + kP_Z = \text{constant} \tag{5}$$

Furthermore, the components, and hence, P_X^2, P_Y^2, and P_Z^2 are each constant. Thus,

$$P^2 = P_X^2 + P_Y^2 + P_Z^2 = \text{constant} \tag{6}$$

In books on classical mechanics, it is shown that the value of P^2 is independent of the coordinate system employed; hence,

$$P^2 = P_x^2 + P_y^2 + P_z^2 = \text{constant} \tag{7}$$

It is also shown that when no torque is applied, the kinetic energy of rotation remains constant.

$$E_r = \tfrac{1}{2}\left(\frac{P_x^2}{I_x} + \frac{P_y^2}{I_y} + \frac{P_z^2}{I_z}\right) = \text{constant} \tag{8}$$

However, the individual components in the body-fixed axes, P_x, P_y, and P_z, may not be constant.

The characteristic energy levels required for finding the microwave spectral frequencies of a molecule are eigenvalues of the Hamiltonian operators, which are usually expressed in terms of the angular momentum operators of a particle or system of particles. The matrix elements of these angular momentum operators are, therefore, useful in finding the characteristic energies of the system, i.e. the eigenvalues of the Hamiltonian operator. The classical angular momentum of a system of particles can be expressed by $P = \Sigma r_n \times p_n$, where p_n is the instantaneous linear momentum $m_n v_n$ of the nth particle and r_n is its radius vector from the center of rotation, assumed to be fixed in space. Expanded in terms of its components in space-fixed rectangular coordinates X, Y, and Z, it is

$$\begin{aligned} P &= \hat{i}P_X + \hat{j}P_Y + \hat{k}P_Z \\ &= \Sigma_n \left[\hat{i}(Y_{P_Z} - Z_{P_Y})_n + \hat{j}(Z_{P_X} - X_{P_Z})_n + \hat{k}(X_{P_Y} - Y_{P_X})_n\right] \end{aligned} \tag{9}$$

To derive the corresponding quantum mechanical angular momentum operators, one substitutes the relations $P_X \rightarrow (\hbar/i)(\partial/\partial X)$, etc. It can then be shown that $\hat{P}^2$ commutes with its component operators (Ref. 1, p. 174), e.g.,

$$\hat{P}^2 P_Z - \hat{P}_Z \hat{P}^2 = 0 \tag{10}$$

The component operators do not commute among themselves, however. The following commutation rules are easily shown to hold

$$\hat{P}_X \hat{P}_Y - \hat{P}_Y \hat{P}_Z = i\hbar \hat{P}_Z$$

$$\hat{P}_Y\hat{P}_Z - \hat{P}_Z\hat{P}_Y = i\hbar\hat{P}_X$$

$$\hat{P}_Z\hat{P}_X - \hat{P}_X\hat{P}_Z = i\hbar\hat{P}_Y \tag{11}$$

The important commutation relations for the components can be expressed more compactly by the vector equation

$$\hat{\vec{P}} \times \hat{\vec{P}} = i\hbar\hat{\vec{P}} \tag{12}$$

It is one of the principles of quantum mechanics that operators which commute have common sets of eigenfunctions. Therefore, $\hat{P}^2$ and $\hat{P}_Z$ have common eigenfunctions, which we designate $\psi_{J,M}$. By means of various manipulations based on the commutation relations, it can be shown that (Ref. 2)

$$\hat{P}^2\psi_{J,M} = \hbar^2 J(J + 1)\psi_{J,M} \tag{13}$$

$$\hat{P}_Z\psi_{J,M} = \hbar M\psi_{J,M} \tag{14}$$

where

$$J = 0,1,2,3...\text{and } M = J,J - 1, J - 2,... -J \tag{15}$$

From Eqs. (13) and (14) it is evident that the nonvanishing matrix elements of P^2 and P_Z are

$$(J,M/\hat{P}^2/J,M) = \hbar^2 J(J + 1) \tag{16}$$

$$(J,M/\hat{P}_Z/J,M) = \hbar M \tag{17}$$

It is, of course, always true that the matrix of an operator in the representation of its eigenfunctions is diagonal.

The operators $\hat{P}_X$ and $\hat{P}_Y$ are not diagonal in the J,M representation because they do not commute with $\hat{P}_Z$. Since $\hat{P}_X$ or $\hat{P}_Y$ commutes with $\hat{P}^2$, we could have chosen a set of eigenfunctions common to $\hat{P}^2$ and $\hat{P}_X$, or to $\hat{P}^2$ and $\hat{P}_Y$, but then the matrix elements of $\hat{P}_Z$ would not have been diagonal in either of these representations. The choice of the particular pair $\hat{P}^2$ and $\hat{P}_Z$ is completely arbitrary. From algebraic manipulations involving the commutation relations and the condition that the quantum mechanical operators of all physically real quantities must be Hermitian, the nonvanishing matrix elements of $\hat{P}_X$ and $\hat{P}_Y$ in the J,M representation are found to be (Ref. 3)

$$(J,M/\hat{P}_Y/J,M \pm 1) = \pm (\hbar/2)\,[J(J+1) - M(M \pm 1)]^{1/2}$$

$$(J,M/\hat{P}_X/J,M \pm 1) = \pm (\hbar/2)\,[J(J+1) - M(M \pm 1)]^{1/2} \qquad (18)$$

These elements are seen to be diagonal in J, but not in M.

For the symmetric-top rotor, one of the principal axes lies along the symmetry axis of the top. It is customary to designate this as the z axis, so that for the symmetric top we have $I_x = I_y$. By substitution of this relation into Euler's equations of motion, one obtains

$$\frac{dP_z}{dt} = 0, \text{ hence, } P_z = \text{constant} \qquad (19)$$

P_x and P_y are not constants of the motion of a symmetric top. For the asymmetric rotor $I_x \neq I_y \neq I_z$, there is, in contrast, no internal axis about which the rotation is constant, although P^2 is a constant for the asymmetric rotor and is independent of the coordinate system in which it is expressed.

2.2 SYMMETRIC-TOP MOLECULES

For the symmetric top, the operator $\hat{P}_z$ will commute with $\hat{P}^2$ since both are constants of the motion. Furthermore, $\hat{P}_Z$ still commutes with $\hat{P}^2$ since the latter is independent of the coordinate system employed. Thus, both $\hat{P}_Z$ and $\hat{P}_z$ commute with $\hat{P}^2$, and hence, with each other and have a common set of eigenfunctions, $\psi_{J,K,M}$. The eigenvalues of P^2 can be found from the commutation rules of the angular momentum operators expressed in the internal coordinate system. Those rules are similar to those for the space-fixed system except for a change in the sign of i. In this system, $\hat{P}_z$ commutes with $\hat{P}^2$, and

$$\hat{\vec{P}} \times \hat{\vec{P}} = -i\hbar\,\hat{\vec{P}} \qquad (20)$$

From these rules, the eigenvalues of $\hat{P}_z$ are found to be Kh, where K is an integer equal to, or less than, J (Ref. 4). Thus, for the symmetric top we have the additional set of diagonal matrix elements,

$$(J,K,M/\hat{P}_3/J,K,M) = K\hbar \qquad (21)$$

where

$$K = J, J-1, J-2, \ldots -J \qquad (22)$$

The matrix elements of $\hat{P}_x$, $\hat{P}_y$, and $\hat{P}_z$ in the body-fixed system are independent of M, but we retain the M subscript to indicate the common eigenfunction.

$$(J,KM,/\hat{P}\ /J,K \pm 1,M) = \pm i\frac{\hbar}{2}\Big[J(J+1) - K(K \pm 1)\Big]^{1/2}$$

$$(J,K,M/\hat{P}\ /J,K \pm 1,M) = \frac{\hbar}{2}\Big[J(J \pm 1) - K(K \pm 1)\Big]^{1/2} \tag{23}$$

The Hamiltonian operator is obtained from the classical Hamiltonian when the momenta are replaced by their conjugate operators. When no torques are applied, the classical Hamiltonian of the rigid rotor consists of only kinetic energy which can be expressed in terms of the components of angular momentum in the principal axes, as in Eq. (4). To find the corresponding Hamiltonian operator, one simply substitutes for the P's the conjugate angular momentum operators. In the body-fixed principal axes, x,y,z, this operator is

$$\hat{H}_r = \tfrac{1}{2}\left(\frac{\hat{P}_x^2}{I_x} + \frac{\hat{P}_y^2}{I_y} + \frac{\hat{P}_z^2}{I_z}\right) \tag{24}$$

where

$$\hat{P}_x = \frac{\hbar}{i}\left(y\frac{\partial}{\partial z} - z\frac{\partial}{\partial y}\right), \text{ etc.}$$

The eigenvalues of the Hamiltonian operators represent the quantitized energies from which the microwave spectral frequencies are determined. In the rigid rotor approximation, the Hamiltonian operators are expressed in terms of angular momentum operators, and the matrix elements of angular momentum operators are used when finding the energy levels involved in microwave spectral transitions. Effects such as centrifugal distortion, rotational-vibrational interaction, internal rotations, and externally applied electric or magnetic fields are treated as perturbations of the rigid rotor energies.

If the Hamiltonian operator is found to commute with the angular momentum operators, it will be diagonal in the representation in which these operators are diagonal. Its matrix elements can then be found from the known diagonal matrix elements of the angular momentum operators.

For example, the Hamiltonian operator of the symmetric-top rotor commutes with $\hat{P}_Z$ and $\hat{P}_z$ as well as with $\hat{P}^2$ and is, therefore, diagonal in the J, K, M representation. This can easily be seen if I_x is set equal to I_y in Eq. (24); the Hamiltonian for the symmetric top can then be expressed as

$$\hat{H}_r = \frac{\hat{P}^2}{2I_y} + \left(\frac{1}{2I_z} - \frac{1}{2I_y}\right)\hat{P}_z^2 \tag{25}$$

Since $\hat{P}^2$ and $\hat{P}_z^2$ are diagonal in the J, K, M representation, $\hat{H}_r$ is also diagonal in the same representation, with matrix elements

$$E_{J,K} = (J,K,M/\hat{H}/J,K,M) = \frac{\hbar^2}{2}\left[\frac{J(J-1)}{I_y} + \left(\frac{1}{I_z} - \frac{1}{I_y}\right)K^2\right] \tag{26}$$

which represent the characteristic rotational energies.

A molecule in which two of the principal moments of inertia are equal is a symmetric-top rotor. This condition is generally met when the molecule has an axis of symmetry which is trigonal or greater. Classically, the molecule rotates about the symmetry axis while this axis in turn precesses about a fixed direction in space corresponding to the direction of the total angular momentum P. One of the principal axes of inertia must lie along the molecular axis of symmetry. The principal moments of inertia which have their axes perpendicular to this axis are equal. If a, the axis of least moment of inertia ($I_a < I_b = I_c$), lies along the symmetry axis, the molecule is a prolate symmetric top. If c, the axis of greatest moment of inertia ($I_a = I_b < I_c$), lies along the symmetry axis, the molecule is an oblate symmetric top. Most of the symmetric-top molecules observed in the microwave region are prolate. With the a axis chosen along the symmetry axis ($I_a = I_b$) and with $\hat{P}^2 = \hat{P}_a^2 + \hat{P}_b^2 + \hat{P}_c^2$, the Hamiltonian of Eq. (25) may be expressed as

$$\hat{H}_r = \frac{\hat{P}^2}{2I_b} + \frac{1}{2}\left(\frac{1}{I_a} - \frac{1}{I_b}\right)\hat{P}_a^2 \tag{27}$$

In the a, b, c system used here for designation of the principal axes of inertia, z becomes a for the prolate top, and z becomes c for the oblate top. In the field-free rotor, the rotational energies do not depend on m. The Hamiltonian operator of Eq. (27) commutes with $\hat{P}^2$ and $\hat{P}_a$ and is, therefore, diagonal in the J, K representation. Its eigenvalues, which are the quantized rotational energies of the rigid prolate symmetric top are, therefore,

$$E_{J,K} = \frac{h^2}{8\pi^2 I_b} J(J+1) + \frac{h^2}{8\pi^2}\left(\frac{1}{I_a} - \frac{1}{I_b}\right)K^2 \tag{28}$$

With the designation $A = h/(8\pi^2 I_a)$ and $B = h/(8\pi^2 I_b)$, $E_{J,K}$ can be written

$$E_{J,K} = h[BJ(J+1) - (A-B)K^2] \tag{29}$$

Although K can have both positive and negative values, the + and − values do not lead to separate energy levels. Thus, all K levels except those for K = 0 are doubly degenerate. This K degeneracy cannot be removed by either external or internal fields. In addition to the K degeneracy, there is a (2J + 1) M degeneracy in the field-free symmetric rotor. Unlike the K degeneracy, the M degeneracy can be lifted completely by the application of an external electric or magnetic field.

The transition probabilities for induced absorption are proportional to the squared dipole-moment matrix elements with reference to the space-fixed axis as expressed by the Einstein B coefficient (Ref. 2, p. 30)

$$B_{J,K,M \rightarrow J',K',M'} = \frac{8\pi^3}{3h^2} \sum_{F = X,Y,Z} \left| (J,K,M \left| \mu_F \right| J',K',M') \right|^2 \qquad (30)$$

where μ_X is the component of the permanent dipole moment of the molecule resolved along the space-fixed X axis, etc. This equation provides the basis for the selection rules of dipole absorption and is a factor in the calculation of intensities of spectral lines. The pure, rotational transitions observed in the microwave region do not generally change the electric dipole moment of the molecule; therefore, we can treat the electric dipole components in the rotating, body-fixed system as constants. The problem is to find the nonvanishing matrix elements resolved on space-fixed axes in the representation which diagonalizes the Hamiltonian operator. We can choose the body-fixed dipole components along the principal axes of inertia. Then, for example, a molecule with constant dipole moment components in the body-fixed principal axes of μ_x, μ_y, μ_z would have components along the space-fixed Z axes of

$$\mu_Z = \mu_x \phi_{Zx} + \mu_y \phi_{Zy} + \mu_z \phi_{Zz} \qquad (31)$$

where ϕZx is the cosine of the angle between the Z and x axes, etc. The direction cosine matrix elements have been evaluated and tabulated in the symmetric-top representation, J,K,M (Ref. 5). In symmetric-top molecules only μ_z is nonzero. Electric dipole transitions occur only between levels for which the matrix elements of μ_X, μ_Y, and μ_Z do not all vanish. In this way, the selection rules for the symmetric top are found to be

$$\Delta J = 0, \pm 1 \quad \Delta K = 0 \quad \Delta M = 0, \pm 1 \qquad (32)$$

In the absence of a permanent electric field, the energy levels do not depend on M, and the $\Delta M = 0, \pm 1$ rule does not apply. The rule corresponding to absorption of radiation is $J \rightarrow J + 1$ and $K \rightarrow K$. Application of these rules to Eq. (29) gives the formula for the absorption frequencies of the symmetric top in the absence of centrifugal stretching,

$$\nu = 2B(J + 1) \tag{33}$$

However, centrifugal stretching separates the lines corresponding to different $|K|$ by frequencies which are small but usually resolvable in a microwave spectrum taken at low pressure.

2.3 ASYMMETRIC-TOP MOLECULES

When no two of the three principal moments of inertia of a molecule are equal, much greater complexity results in its pure, rotational spectrum. Only for certain low-J values can the energy levels of the asymmetric rotor be expressed in closed form, even when centrifugal distortion is neglected. The Hamiltonian operator for the asymmetric-top does not commute with $\hat{P}_z$, $\hat{P}_x$, or $\hat{P}_y$, and is, thus, not diagonal in the symmetric-top J,K,M representation. The general procedure is to assume that the wave functions can be expanded in terms of the symmetric-top functions and to set up the secular equation for the unknown coefficients and energies. The resulting secular determinant is diagonal in J and M, but not in K, and may be broken down into subdeterminants for each value of J.

In order to understand the energy levels and selection rules for asymmetric-top molecules, one must first become familiar with the notation used to designate the levels. There is no longer an internal component of angular momentum which is a constant of the motion, i.e., $\hat{P}_z$ does not commute with $\hat{H}$; and K, which gives the projection of the angular momentum along the z axis, is no longer a "good" quantum number, though J and M are still good. The Hamiltonian describing the motion of a rigid asymmetric body is

$$\hat{H} = A\hat{P}_a^2 + B\hat{P}_b^2 + C\hat{P}_c^2 \tag{34}$$

with A, B, and C defined as before and the P's representing the angular moments. The calculation of energy levels is facilitated by the following rearrangement:

$$\hat{H} = \frac{1}{2}(A + C)\hat{P}^2 + \frac{1}{2}(A - C)\hat{H}(x) \tag{35}$$

$$\hat{H}(x) = \hat{P}_a^2 + x\hat{P}_b^2 - \hat{P}_c^2 \tag{36}$$

$$x = \frac{2B - A - C}{A - C} \tag{37}$$

The dimensionless number x, known as Ray's asymmetry parameter, gives a measure of the degree of asymmetry. The most asymmetric top has $x = 0$, while the limiting values of -1 and 1 correspond to prolate and oblate symmetric tops, respectively. The energy levels of slightly asymmetric rotors ($x \approx -1$ or ≈ 1) differ from the limiting symmetric-top ones only in that levels corresponding to $-K$ and K are separated in the asymmetric rotor.

The matrix elements of $\hat{H}(x)$ in the symmetric rotor basis are given in closed form by rather complex algebraic equations. The energies $E_J(x)$ are found by diagonalizing the submatrix of the secular determinant that corresponds to each value of J. The total rotational energy for a particular level is then given by (Ref. 6)

$$E = \frac{1}{2}(A + C)J(J + 1) + \frac{1}{2}(A - C)E_{J_\tau}(x) \tag{38}$$

where J_τ is a "pseudoquantum" number whose value ranges from $-J$ to J in order of increasing energy. A more common means of designating the asymmetric-top sublevels involves following each sublevel as one imagines the shape of the molecule to continuously evolve into prolate and oblate tops. The K value for the limiting prolate top is designated K_{-1}, and the K value for the limiting oblate top K_1. The energy levels are then labeled by $J_{K_{-1}K_1}$. This notation is related to the single subscript τ by

$$\tau = K_{-1} - K_1 \tag{39}$$

As for the symmetric top, the allowed changes in J for dipole absorption of radiation by asymmetric tops are

$$\Delta J = 0, \pm 1 \tag{40}$$

This is to be expected since the asymmetric rotor wave functions are expressed as linear combinations of the symmetric rotor functions, all having the same value of J. In a symmetric rotor, the level with higher J always has higher energy; however, in an asymmetric rotor, each of the three changes might give rise to an absorption line. As in infrared work, the $\Delta J = -1$ transitions are designated as P branch; the $\Delta J = 0$, as Q branch; and the $\Delta J = 1$ as R branch transitions.

In addition to the above selection rules for J, there are also restrictions on the changes which can occur in the pseudoquantum numbers K_{-1} and K_1. The allowed transitions are those for which the matrix elements of the dipole moment are nonvanishing. An asymmetric

top may have a component of its dipole moment along each of the three principal axes of inertia, and each component leads to a different set of selection rules. In terms of permitted changes in the K_{-1} and K_1 subscripts, the selection rules are (Ref. 7)

	ΔK_{-1}	ΔK_1
$\mu_a \neq 0$		
(along axis of least moment of inertia)	0, ±2,...	± 1, ± 3,...
(along axis of intermediate moment of inertia)		
$\mu_c \neq 0$	± 1, ± 3,...	± 0, ± 2,...
(along axis of greatest moment of inertia)		

(41)

Any given transition will be attritutable to only one component of the molecular dipole. The transition will be because of the μ_a component and are designated as "a-type" transitions, etc. If one dipole-moment component is much larger than the other two, then transitions of that type will result in much stronger absorption lines. While any changes indicated in the previous table are permitted by the selection rules, the strongest lines always correspond to the smallest changes in both subscripts. Futhermore, if the rotor is near the limiting prolate symmetric-top case ($K = -1$), the changes in K_{-1} which correspond to the symmetric-top selection rule $\Delta K_{-1} = 0$ will be the only ones of significant strength.

2.4 EFFECT OF AN APPLIED ELECTRIC FIELD AND STARK MODULATION SPECTROMETERS

The degeneracy of the rotational energy levels with M, which indicates the projection of the dipole moment along a fixed direction in space, is removed by the applications of a constant electric field. Each level corresponding to particular values of J and K will be split into (2J + 1) sublevels. Because this effect is known as the Stark effect after its discoverer, a constant electric field is known as a Stark field. The Stark effect also removes the $|K|$ degeneracy of the symmetric-top levels. In the presence of an external electric field, the transitions are governed by the additional selection rule $\Delta M = 0, \pm 1$. The $\Delta M = 0$ transitions are observed when the constant electric field is parallel to the electric vector of the microwave radiation, and the $\Delta M \pm 1$ lines arise when the two electric fields are perpendicular. The Stark field is usually employed parallel to the radiation field so that only $\Delta M = 0$ transitions are observed (Ref. 8).

For symmetric-top molecules with $K \neq 0$, the energy shifts are calculated by first-order perturbation theory. In this case, one needs to apply only a few hundred volts/centimeter to

obtain a separation of 100 MHz or more among the (2J + 1) Stark components. For the K = 0 symmetric-top levels, and for all levels of the asymmetric top, the shift in frequency arises only in the second order, and is 10 to 100 times smaller than the first-order effect. Thus, for asymmetric tops, one often finds it necessary to apply several thousand volts/centimeter in order to clearly resolve each transition. A completely resolved spectral line with $\Delta J = \pm 1$ will have (J + 1) Stark components; whereas for $\Delta J = 0$, there will be J components.

The Stark effect is frequently used in microwave spectrometers to modulate the detected signal. If the source of radiation is tuned to the frequency of an absorption line in the absence of an electric field, then the application of an electric field will increase the power at the detector, since the Stark components of the line are shifted relative to the source frequency. Thus, high-frequency modulation can be obtained by subjecting the gas to a periodically interrupted electric field, resulting in an amplitude modulation of the signal from the detector. Square-wave modulation is almost universally used with Stark spectrographs, with a phase-sensitive, lock-in amplifier tuned to the modulation frequency.

2.5 LINE STRENGTHS

The inherent ability of a molecule to absorb radiation at a particular frequency is described by the absorption coefficient α defined by

$$\alpha = -\frac{1}{P}\left(\frac{\Delta P}{\Delta X}\right) \tag{42}$$

where ΔP represents the power absorbed in a path length ΔX when the total incident power is P. From time-dependent perturbation theory, one may calculate the Einstein coefficient of stimulated absorption or stimulated emission to be as given by Eq. (30). Under conditions of thermal equilibrium, it is easily shown that for absorption of a photon of energy $h\nu_{mn}$, leading to a transition from a lower level m to a higher level n (Ref. 9)

$$\alpha_{mn} = \frac{NF_m}{c}\left(1 - e^{-h\nu mn/kt}\right)B_{mn}h\nu_{mn} \tag{43}$$

The Einstein coefficient of spontaneous emission, which is proportional to ν^3, can be neglected at microwave frequencies. N represents the number of molecules per unit volume and F_m, the fraction of the molecules in the state m. At microwave frequencies and ambient temperature, $h\nu/kT$ is on the order of 10^{-3}, and the quantity in brackets may be replaced by $h\nu_{mn}/kT$. The absorption coefficient for isotropic radiation of any frequency ν under conditions of thermal equilibrium can be found from Eq. (43) upon multiplication by the properly normalized line shape function $S(\nu,\nu_o)$.

At the pressures usually employed in the measurement of microwave spectral lines, 1 mtorr to 1 torr, pressure broadening arising from the binary collisions of the molecules is the predominant line-broadening factor. At those low pressures, collision-broadened lines have the Lorentzian-shape function

$$S(\nu, \nu_o) = \frac{1}{\pi} \frac{\Delta\nu^2}{(\nu_o - \nu)^2 + (\Delta\nu)^2} \tag{44}$$

where $\Delta\nu$ is the half-width of the line measured at half-intensity. For the maximum absorption of microwave power when $\nu = \nu_o$,

$$\alpha_{max} = \frac{8\pi^2 N F_m \nu_o^2 \left|(m \mid \mu \mid n)\right|^2}{3cKT(\Delta\nu)} \tag{45}$$

For gaseous samples,

$$N = 9.68 \times 10^{18} p/T \tag{46}$$

where p is the pressure in torr. Over the range of very low pressures, the mean collision time τ varies inversely as the pressure. Therefore, $\Delta\nu$ increases with pressure, and we may write

$$\Delta\nu \approx 300p \frac{(\Delta\nu)_1}{T} \tag{47}$$

where $(\Delta\nu)_1$ is the line width measured at T = 300 K and 1 torr of pressure (Ref. 10). Typically, $(\Delta\nu)_1$ falls in the range 9 to 30 Hz. Since the number of absorbing particles also increases linearly with pressure, the peak absorption coefficient, α_{max}, is independent of the pressure; whereas the line width is directly proportional to the pressure.

The fractional part F_m of the particles in state m with degeneracy g_m is

$$F_m = \frac{g_m e^{-Em/kT}}{Q} \tag{48}$$

where Q is the partition function,

$$Q = \sum_i g_i e^{-E_i/kt} \tag{49}$$

The partition function for free gaseous molecules is a function of the electronic, vibrational, rotational, and the nuclear-spin states. If interactions between these various states are neglected, they can be expressed as the product

$$Q = Q_e Q_v Q_r Q_n \tag{50}$$

Most stable organic molecules at ordinary temperatures are in the ground electronic state, and for them we can set $Q_e = 1$. It is convenient to write $F_m = F_v F_r$, where F_v is the fraction of molecules in a particular vibrational state, usually the ground state, and F_r is the fraction in a particular rotational state. Nuclear-spin statistics are included in F_r.

The fraction of molecules in a given vibrational state specified by the set of quantum numbers $v_1, v_2, v_3, \ldots = V$, at a temperature T, is

$$F_v = d_v e^{-h\Sigma_j \nu_j \omega_j / kT} \left(1 - e^{-h\omega/kT}\right)^{d_1} \left(1 - e^{-h\omega/kT}\right)^{d_2} \tag{51}$$

The fraction $F_{J,i}$ of molecules in the rotational state (J,i) with rotational energy $E_{J,i}$ and in vibrational state v is given by

$$F_{J,i} = \frac{F_u g_J g_i e^{-E_{Ji}/kT}}{Q_r} \tag{52}$$

where

$$Q = \sum_{Ji} \sum g_j g_i e^{-E_{J,i}/kT} \tag{53}$$

Here i signifies any internal quantum numbers such as K of the symmetric top. The degeneracies $g_J = 2J + 1$ associated with the quantum number M are the same for all classes of molecules. This degeneracy is removed by the application of an external electric field. The degeneracy factor g_i is that associated with all inner quantum numbers and includes, in addition to the K degeneracy of the symmetric top, all degeneracies caused by nuclear spins, inversion, and internal rotation. Usually, however, the inversion and internal rotation degeneracies are the same for the different levels and cancel from the ratio g_i/Q_r. Except for linear molecules and symmetric tops having certain symmetries, the effects of nuclear spins also cancel from the ratio g_i/Q_r and need not be included in either. Any nuclear hyperfine splitting of the levels can be neglected in the calculation of the integrated population of the rotational level. In particular, there are no hyperfine splitting or nuclear-spin degeneracies in the energy levels of the ethylene glycol molecule.

For an asymmetric-top molecule, the fraction of molecules in a given rotational state J_τ can be expressed as

$$F_{J_\tau} = \frac{F_v(2J + 1)}{Q_r} e^{-E_{J,J_\tau}/kT} \tag{54}$$

where E_{J,J_τ} is the energy above the ground state.

An approximate formula for the partition function of the asymmetric rotor is

$$Q_r = \frac{5.34 \times 10^6}{\sigma} \frac{T^{3/2}}{(ABC)^{1/2}} \tag{55}$$

where the spectral constants A, B, and C are in megahertz units and the summetry number σ is defined as the number of indistinguishable positions of the nuclei which can be achieved through simple rotation of the rigid molecule. For molecules without such symmetry, such as ethylene glycol, $\sigma = 1$.

One further factor in the expression for the absorption coefficient of asymmetric tops that needs to be discussed is the dipole-moment matrix elements $(J, \tau/\mu/J', \tau')/$. As indicated by the selection rules, each component μ_g of the dipole moment along the principal axes corresponds to a different set of transitions. The absorption coefficient for a particular transition depends only on the appropriate component of the dipole moment. For a transition casused by a component of the electric moment μ_g, a convenient quantity called the "line strength" is defined as

$$\lambda_g(J, \tau, J', \tau) = \sum_{FMM'} \left| (J, \tau, M \left| \phi_{Fg} \right| J', \tau', M') \right|^2 \tag{56}$$

where the sum extends over the three directions of the space-fixed system and over all values of M and M'. Extensive tables of line strengths for various values of K are available from the National Bureau of Standards (Ref. 3). The dipole matrix element appearing in Eq. (45) for the absorption coefficient is related to the line strength as follows (Ref. 2, p. 195)

$$\left| (J,\tau \left| \mu \right| J',\tau') \right|^2 = \frac{\mu_g^2 \lambda_g(J, \tau, J', \tau'}{(2J + 1)} \tag{57}$$

If Eq. (57) and Eqs. (47), (54), and (55) are inserted into Eq. (45), the peak absorption coefficient for the transition $J,J_\tau \rightarrow J', J_\tau'$ may be written as

$$\alpha_{max} = 3.85 \times 10^{-14} F_v (ABC)^{1/2} \mu_g^2 \lambda_g(J,\tau,J',\tau') \left(\frac{\nu_o^2}{(\Delta\nu)_l T^{5/2}} \right) e^{-E_{J,\tau}/kT} \quad (58)$$

where it is assumed that $\hbar\nu_o \ll kT$. The rotational constants A, B, and C, the resonant frequency ν_o, and the line width $(\Delta\nu)_l$ are in megahertz, with μ_g in Debye units and α_{max} in cm^{-1}.

3.0 SPECTRA OF ETHYLENE GLYCOL

The conformation and structure of the free ethylene glycol molecule (CH_2OH-CH_2OH), as well as its internal motions, have been the subject of experimental and theoretical investigations over the last 40 years (see Ref. 4 and references therein). Rotation about the central C-C bond is possible, but in addition, the two hydroxyl groups can rotate internally. Furthermore, an intermolecular hydrogen bond forms between the two oxygen atoms. The possible stable conformers of gylcol have been studied by ab initio quantum mechanical calculations. Two different hydrogen-bonded gauche conformations (with dihedral angle near 60 deg) were reported to be the most stable conformers. Experimental investigations involving such techniques as electron diffraction, infrared spectra in the gas, liquid, and solid phase, and the infrared spectra of species in the gas, liquid, and solid phase, and the infrared spectra of species isolated in Ar and Xe matrices have yielded results consistent with a hydrogen-bonded gauche conformation.

The most thorough study of the microwave spectrum was done by Marstokk and Mollendal (Ref. 11) who measured over 600 medium and strong transitions in the 8- to 38-Ghz spectral region. Attempts to fit these lines to a rigid rotor spectrum of a gauche conformer proved impossible. The confusing nature of the spectrum results from the large splitting of each line because of tunneling motion in a double minimum potential because of the simultaneous rotation of the two hydroxyl hydrogens. Their measured absorption frequencies are found in Appendix A. One interesting feature of this spectrum is that more than 200 of the strongest lines fall in the 16- to 19-GHz range with a large pile-up of lines near 17.1 GHz. Since the lines could not be assigned, it is impossible to calculate the strength of the absorption for a transition.

The structure of ehtylene glycol has been clarified by studies of deuterated species. Walder et al. (Ref. 4) investigated the microwave spectrum of a dideuterated form of ethylene glycol (CH_2OD-CH_2OD) in the frequency range from 18 to 50 GHz. The hydrogen bond is much stronger in this case because of the "Ubbelhode" effect, that is, the shrinkage upon deuteration of the distance between the two heavy atoms involved in the hydrogen bond. Because this limits the internal rotation of the hydroxyl groups, there is much smaller

splitting of the rigid rotor energy levels, and they were able to assign many of their observed transitions. They found that their data were consistent with a gauche conformation that has the free-hydroxyl transitions with respect to the C-C bond, and a splitting of the rotational levels of 550 to 590 MHz. However, despite the detailed spectral data available, they could neither determine the accurate structure of the observed conformer, nor exclude the presence of more than one conformer. On the basis of their very detailed theoretical model, these authors predict that the transitions in the undeuterated form would show a splitting of 30 to 40 GHz, rendering assignments of the microwave spectrum virtually impossible.

Recently, Caminati and Corbelli (Ref. 5) reported a study of the rotational spectrum of the nontunneling 0-monodeuterated species in the range 8 to 54 GHz. Because the symmetry of the molecular structure is broken in this species, there is no splitting of the rotational energy levels attributable to the concerted internal rotation of the hydroxyl groups. Their data were consistent with a gauche conformation with the free-hydroxyl transitions as shown in Fig. 2.

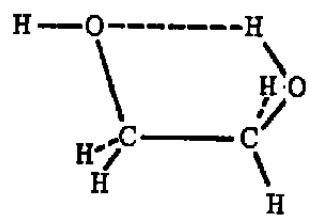

Figure 2. Most likely conformer of ethylene glycol.

The best estimate of the rotational constants of ethylene glycol is that used by Marstokk and Mollendal (Ref. 11), A = 16.4 GHz, B = 5.1 GHz, and C = 4.4 GHz. The value of the asymmetry parameter is $\kappa = -0.81$, which is also the value in the more accurately known dideuterated species. As for the dipole moment, the most accurate values are those of Walder et al. (Ref. 4) for the dideuterated species, $\mu_a = 2.166(37)$, $\mu_b = 0.74(18)$, and $\mu_c = 0.75(21)$, where the values are in Debye units. These values are consistent with the various ab initio calculations done on the undeuterated species.

Because the dipole moment is nearly parallel to the axis of least moment of inertia, a-type transitions will give the strongest absorption lines. Though no prediction can be made as to where the strongest absorption lines occur in the spectrum, a prediction can be made of the absorption coefficient of the strongest lines. Though the general spectrum of a molecule as asymmetric as ethylene glycol is rather chaotic, it is near enough to being a prolate top ($\kappa = -0.81$) that the strongest rigid rotor lines occur in a clear pattern. The strongest lines are those for which $\Delta j = 1$, $\Delta K_{-1} = 0$, and $\Delta K_1 = 1$. These lines correspond to the parallel-type transitions of the symmetric top ($\Delta J = 1$, $\Delta K = 0$), each of which is split into $(2J + 1)$ lines

by the asymmetry of the molecule. For ethylene glycol, they would occur over a range of about 2.7 GHz at 30 GHz (J = 2) and over a range of about 13 GHz at 150 GHz (J = 14), with the strongest lines, corresponding to the lowest values of K_{-1}, occurring at the lower frequency end of the range.

In calculating the absorption coefficient from Eq. (58), it was assumed that T = 300 K and μ_a = 2.10. The line strengths were obtained from the National Bureau of Standards table of line strengths for asymmetric rotors. The fraction of molecules in the ground vibrational state F_o was calculated from Eq. (51) and the vibrational frequencies measured by Buckley and Giguere (Ref. 6) (Appendix B). With T = 300 K, F_o = 0.360. The absorption coefficients calculated from Eq. (58) were then reduced by a factor of two, because each rotational transition appears as two widely separated lines. For J = 2 → 3 and $\Delta K_{-k} = 0$ (ν_o = 30 GHz), $\alpha_{max} = 4.5 \times 10^{-6}$ to 8.1×10^{-6} cm^{-1}. For J = 14 → 15 and $\Delta K_{-1} = 0$ ($\nu_o \approx$ 150 GHz), $\alpha_{max} = 7.7 \times 10^{-5}$ to 6.64×10^{-4} cm^{-1}. Furthermore, a number of $\Delta J = 0$ lines have absorption coefficients on the order of the smaller of these values.

Strong absorption lines for ethylene glycol should occur throughout the entire microwave region. In any 5-GHz interval there should be several strong lines that could be used for detection of trace amounts of ethylene glycol. However, the most inexpensive detection schemes would involve a fixed frequency source that had been pretuned to one of the strongest ethylene glycol absorption lines. Such a minimal spectrometer would also be more easily transported and more rugged. In order to employ such a scheme, the exact frequency of a strong line would have to be measured by an outside laboratory before the solid-state source was ordered.

4.0 DETECTION OF ETHYLENE GLYCOL

The complexity and cost of the detection method depends largely on the sensitivity and quantitative accuracy that is desired. There is also the problem that there is no strong absorption line whose frequency is known. Three detection schemes will be outlined, and the source and cost of components given where possible. The first method involves a rapid low-resolution scan over the clump of lines centered at 17.1 GHz. The sensitivity of this technique would be limited, and only very rough quantitative measurements could be made. The other two schemes require prior identification of one of the stronger absorption lines of ethylene glycol and a fixed frequency source tuned to the frequency of a strong absorption. A single spectrometer whose components cost only two or three thousand dollars would be capable of detecting concentrations as low as 10 ppm. The concentration would be roughly proportional to the absorption output. The third section of this chapter describes a

calibration procedure that can be used with an analytical spectrometer. The last section of the report will detail a more sophisticated design that provides for greater sensitivity, quantitative precision, and reliability.

4.1 FAST-SCAN, LOW-RESOLUTION SPECTROMETER

The frequency of many ethylene glycol transitions is known, but not their strength. A scan over a number of lines would likely include some strong ones, and the pattern of lines would be unique to ethylene glycol. Marstokk and Mollendal (Ref. 11) measured 101 lines over a 1-GHz range centered about 17.1 GHz. If this region were repeatedly swept every minute or so (a sweep rate of 10 to 20 MHz/sec), it would yield a distinct spectrum when ethylene glycol was present. A detector time constant of 1 sec or more would result in many of the lines being unresolved. They would thus appear as a single strong absorption. This spectrometer could be operated at a pressure as high as 0.5 torr without loss of sensitivity because of pressure broadening. The absorption cell would be a length of waveguide that is appropriately vacuum sealed at each end. Mylar® or mica sheets serve as strong material with good microwave transmission properties; either of these can be obtained at low cost. The sample gas would be caused to flow continuously through the waveguide cell. Round holes are made in the guide for evacuation of the cell and for introduction of the gas. The diameter of these holes should be small as compared with the wavelength in the guide in order to prevent reflections of the microwaves. A diameter of 1/32 in. would be appropriate at 17 GHz.

A crystal detector, usually a very fine tungsten metal whisker in point contact with a doped silicon single crystal, is used for the continuous detection of microwave radiation at the end of the absorption cell. The function of the detector is to rectify the microwave frequency, thus producing a dc current that is proportional to the incident microwave power. The 1N26 or 1N31 crystals are appropriate for use at 17 GHz. The crystal is mounted along the inner conductor of a coaxial line shorted at one end. Thus, the waveguide mounts must provide a waveguide-to-coaxial transition. Commerical waveguide mounts are available from a number of vendors. In order to maximize the power at the crystal, the waveguide should be terminated by a movable short (Fig. 3). Self-contained microwave detectors are available from the Electron Dynamics Division of Hughes Aircraft Company.

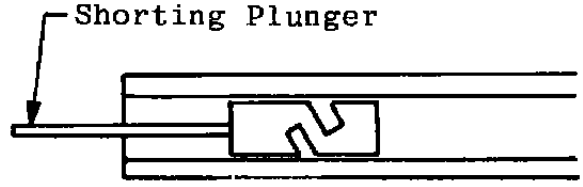

Figure 3. Terminated waveguide.

The waveguide cell should be as long as possible commensurate with portability and available space. The amount of gas exposed to the microwaves, and thus the sensitivity, increases as the cell length. One option would be to coil the waveguide up into a cylindrical shape. Another option would be to machine a spiral-shaped waveguide into a block of metal. A 1-m-long cell could be machined into a block 6 by 6 by 1 in.

As discussed earlier, greatly improved signal-to-noise ratio for a microwave spectrometer may be attained through the use of Stark modulation. As a result of the applied electric field, the normal transition frequency is displaced from the center frequency, ν_0. For detection of transitions in an asymmetric top, a field of up to 2,000 v/cm is needed, requiring a voltage of 1,000 v to be switched on and off in a square-wave manner at rates up to 100 kHz. The high switching rate eliminates 1/f noise because of the modulation.

The usual way to construct a Stark modulation cell is to place a conducting strip down the center of a waveguide section as shown in Fig. 4. This method was first described by Hughes and Wilson (Ref. 7). The conducting strip is held in the center, perpendicular to the E lines, by a dielectric material such as Teflon® which also insulates it from the waveguide walls. Custom-designed waveguide is available commercially from a number of sources. Usually the waveguide is grounded and the modulating voltage applied to the inner conducting strip. During the first half of the cycle of the square wave (V = 0), absorption takes place at the frequency ν_0. During the second half of the voltage cycle, the line is split into its Stark components at other frequencies. Thus, if the microwave frequency is near coincidence with ν_0, the absorption caused by the transition at ν_0 will be chopped at the rate of the applied modulating voltage. The output voltage of the detector crystal is fed into a lock-in amplifier, which is referenced to the modulation frequency, and includes a phase-sensitive detector, so that only signal or noise of the same frequency and phase as the modulation signal appears at its output. For most molecules, a field of 2,000 v/cm is quite adequate for full modulation of the lines. Since the Stark modulator can be a source of interference, it should be enclosed in a metal shield as near to the cell as possible. The modulation should be sent to the waveguide through a shielded cable.

The waveguide of the appropriate size for 17 GHz is known commercially as P band. Its inside dimensions are 0.622 by 0.311 in., and it is the standard waveguide for frequencies from 12.4 to 18.0 GHz. Waveguide, flanges, and vacuum windows are available from many companies. The large electric field needed to fully modulate the pressure-broadened lines can lead to problems with gas breakdown and glow discharge within the cell. To prevent damage to the Stark septum, the pressure should be monitored with a thermocouple gauge to insure a safe pressure range, i.e. a pressure less than 1 mtorr. The intake line should be equipped with a manual throttle valve to control the amount of gas entering the cell. Because a high vacuum is not needed and the cell volume is small, a large, high-vacuum pump is not

needed. Vac Torr markets a pump with a 5-μm base pressure, pumping rate of 20 ℓ/min, and a weight of only 15 lb. Even smaller, lighter pumps may be available from other manufacturers.

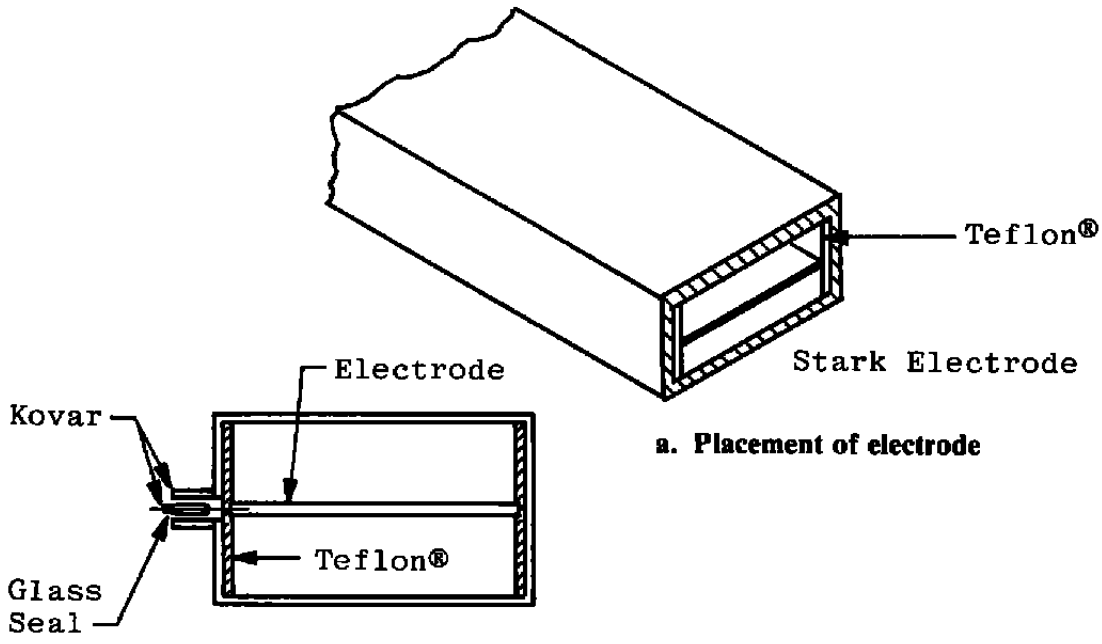

a. Placement of electrode

b. Stark voltage connection

Figure 4. Details of Stark cell construction.

A fully automated source can be purchased from Hewlett Packard Corporation. The HP 8620C mainframe sweep oscillator includes controls that allow for continuous sweeping over any frequency range with the sweep time continuously adjustable from 0.01 to 100 sec. The HP 86260A plug-in provides up to 10 mw of power over the frequency range 12.4 to 18.0 GHz. Plug-in option 001 provides internal leveling. The advantage of internal leveling is that determination of concentration from the strength of the absorption is more accurate when the power from the source remains constant. The power from the source should be adjusted to maximize the response of the detector. A schematic diagram of the spectrometer is shown in Fig. 5. A list of components is found in Appendix C.

The sensitivity of any instrument sampling dilute polar gases in air may be improved through the use of permselective membranes to enrich the concentration of the polar molecule in the air mixture. Permselective membranes such as dimethyl silicone rubber are able to pass some gases at much higher rates than air when a difference in pressure is maintained across the membrane. This property leads to an effective enrichment of a trace component with respect to air at the low-pressure side. The enrichment factor is given by the

ratio of the permeability constant of the trace component to the permeability constant of air, which is

$$30 \times 10^{-9} \frac{\text{cm}^2}{\text{sec cm Hg}} .$$

Water vapor should be kept out of the absorption cell since it leads to increased pressure broadening of the lines. This can be a problem because of the high permeability constant of water, 3,000, which leads to a concentration of the water vapor by a factor of 100. If the airstream being sampled has been predried, this should not be a problem. If water vapor is present in significant amounts, it must be removed by passing the sample through a dryer that selectively removes water vapor. Experiments have shown (Ref. 8) that the dimethyl silicone membrane that serves as the interface between atmosphere and the vacuum system of the Stark cell need only be on the order of 1/4 to 3/8 in. in diameter. These membranes are available from General Electric Corporation.

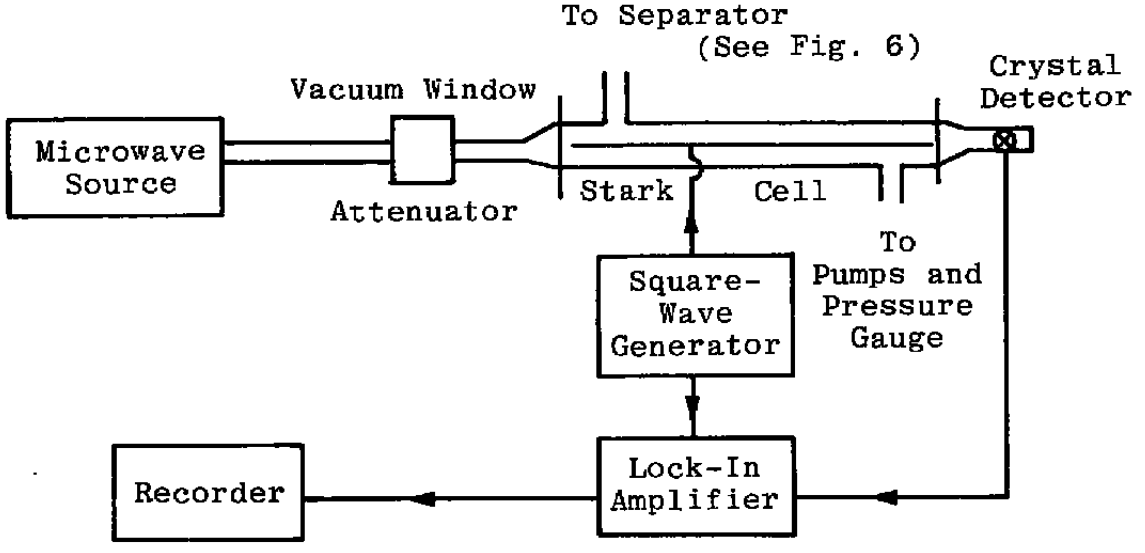

Figure 5. Diagram of Stark modulation spectrometer.

Since the boiling point of ethylene glycol, 198°C, is well above ambient temperature, some of it may condense on the surfaces of the absorption cell and the pumping line. Even for more volatile substances such as formaldehyde, polymerization on available surfaces can be a significant problem. The dire consequence of this effect is that it can cause the instrument to have a long response time, such as taking ten minutes to give a 90-percent response to a sudden increase in trace gas concentration. The severity of this problem for ehtylene glycol can only be determined by testing. Clearly, it is very important to minimize

the length of the line bringing the gas to the absorption cell, regardless of what detection scheme is employed. Tests with other substances have shown that stainless steel should absolutely be avoided. Teflon would probably work best for the pumpting line, and all metal surfaces of the absorption cell should be gold plated. At very low concentrations, handling of any gases becomes increasingly difficult. In many cases, one is forced to use the material showing the best characteristics without understanding why it is better than another. One thing that can be said about inlet systems in general is that if it is necessary to pull the sample into the detector, the wall effects are always very important but poorly understood.

4.2 SIMPLE SPECTROMETER TO DETECT ETHYLENE GLYCOL

Solid-state sources of monochromatic microwave power have recently become available. These tiny sources require only low voltage; in fact they can be battery driven, and they have a power requirement of only a few watts. Thus, the entire source package including the power supply is very small and lightweight compared to backward-wave-oscillator sources such as the Hewlett Packard sweeper described previously. Yet, these solid-state sources are capable of surprising output, as great as 200 mw, far greater than what is needed for a sensitive microwave spectrometer. They also have a very long lifetime.

The most common solid-state source is called a Gunn effect diode. Actually, it is not a diode, but rather a doped GaAs crystal which has a differential negative resistance region in its I-V characteristics that sustains oscillations at microwave frequency. The oscillations from a single Gunn diode can be tuned over a range from a few megahertz to several gigahertz, depending on how it was made. Oscillators of any center frequency, various tuning ranges, and various maximum power outputs are available from a number of manufacturers, including Varian Associates and Hughes Aircraft Corporation. The tuning is usually accomplished electronically by applying a tuning signal to either a varactor (voltage-variable capacitor) or a YIG sphere (ytterbium iron garnet ferrite material) in close proximity to the Gunn diode in a resonant circuit.

Gunn diodes are available for frequencies up to 95 GHz and are known to have low AM and FM noise characteristics. Another type of solid-state source, called an IMPATT diode, is available at frequencies as high as 150 GHz. However, the IMPATT diode is considerably noisier than the Gunn diode. All other considerations being equal, a spectrometer operating at a higher frequency would be more sensitive. The peak absorption coefficient α depends on ν^2, and in addition, the line strength λ_g increases with frequency. For the strongest lines of ethylene glycol, the peak absorption coefficient would be three or four times greater at 145 GHz than at 90 GHz, but this would be more than offset by the increased noise of the source.

The most sensitive microwave analyzer for ehtylene glycol would utilize the strongest absorption line whose frequency coincides with that available from a high-frequency Gunn effect diode.

The simplest spectrometer design is one in which the Gunn diode is used both as an oscillator and detector (Ref. 9). A schematic diagram of the instrument is shown in Fig. 6. A Gunn effect diode and a varacter tuning diode would be positioned side-by-side in a reduced height waveguide which tapers up to full size at the oscillator's RF output. The Gunn diode should be mounted on a bare stud, rather than sealed in the normal commercial package. The waveguide should be shorted with a movable short so that it can be made resonant at the chosen absorption frequency. A vacuum window separates the diodes from the gas in the absorption cell. The gas to be monitored would be sampled continuously by pumping it through a gas-permeable membrane.

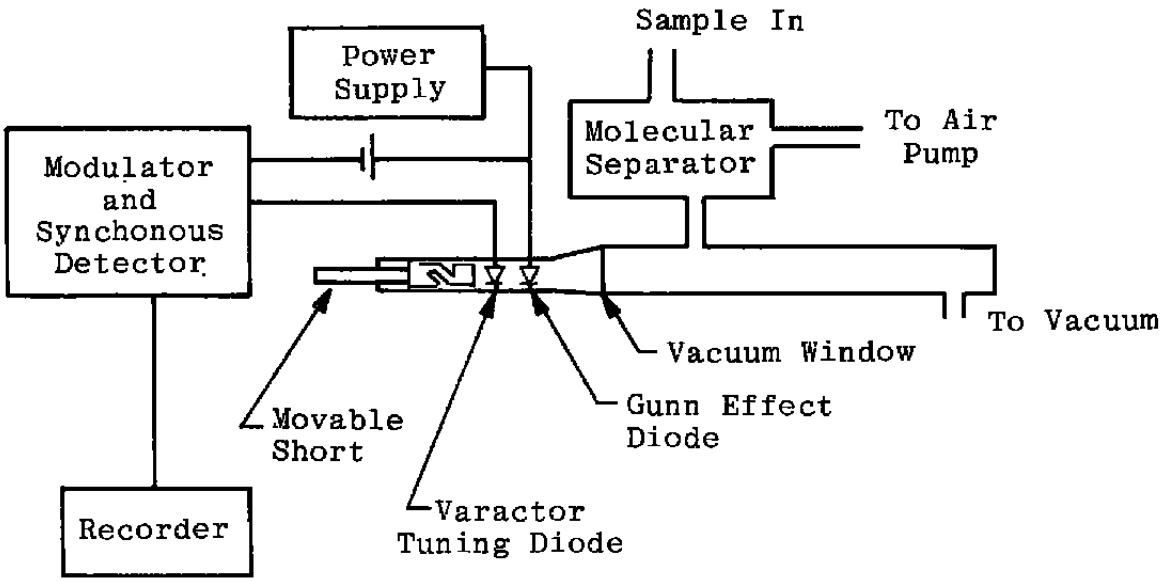

Figure 6. Simple spectrometer for which a Gunn effect diode is both oscillator and detector.

The Gunn diode source is not stable enough to have the output frequency fall right on that of the absorption line each time it is turned on. (The full width at half-power of the absorption line would be a few hundred kilohertz at 50 mtorr of pressure.) The frequency must be swept over a small range to search for the absorption. By applying a tuning voltage to the varactor diode, the resonant frequency of the entire cavity, including the absorption cell, would be made to change over a range of several tens of megahertz. Since the Gunn effect diode oscillates at the resonant frequency of the cavity, the microwave radiation would be simultaneously tuned with the resonant frequency of the cavity. The tuning voltage

could be modulated by a low-frequency sinusoidal signal, such as 250 Hz. Were a gas resonance to be excited within the cavity, a 250-Hz signal would appear on the bias lead to the Gunn diode. The appearance of this signal could be made to activate some sort of indicator to signal the presence of ethylene glycol.

The 250-Hz signal on the Gunn diode lead would be detected synchronously with the 250-Hz reference to obtain a first-derivative signal of the absorption as the frequency is tuned over the line. The output would be fed back to the tuning diode (the varactor) in such a way as to stabilize the oscillator at exact coincidence with the peak center of the gas absorption. Subsequently, another synchronous detection made at twice the 250-Hz frequency would provide a dc output that is proportional to the amount of gas absorbing the microwaves. A spectrometer of this design has been used successfully for several years to detect water-vapor content in pure gases at the Lawrence Livermore Laboratory (Ref. 10). A spectrometer of this type operating in the 80- to 900-GHz range should be capable of detecting concentrations of ethylene glycol as low as 5 to 10 ppm, depending on the strength of the absorption line used and the enrichment achieved by the permselective membrane. A list of the components for this design if found in Appendix C.

4.3 CALIBRATION

The instruments described in Sections 4.1 and 4.2 can be calibrated in the following way. A permeation tube, usually made of Teflon, can be filled with ethylene glycol. If there exists a solid polymer form of ethylene glycol that decomposes readily to give pure ethylene glycol gas, then this would work better. The ethylene glycol gas can permeate the walls of the tube and be flushed by and mixed with air to produce known concentrations of ethylene glycol in the mixture (Ref. 12). With the tube temperature held constant in a controlled oven, the rate of permeation would be constant. If the carrier gas flow rate is also constant, the concentration of ethylene glycol in the mixture would be constant with time. The permeation rate may be determined by measuring the total tube weight loss with time.

Such tubes may be purchased from Dynasciences, Inc., who will provide information on the permeation rates. Only for very accurate quantitative work would the flow rate of the particular tube used to calibrate the instrument need to be checked. The permeation rate can be used to calculate the flow rate from the following equation (Ref. 13):

$$C = \frac{P_r f k}{F} \tag{59}$$

where P_r = permeation rate of $(CH_2OH)_2$ through the tube walls in μg/min/cm;

ℓ = active length of the permeation tube in cm; and

k = Boltzmann's constant

$$F = \left(\frac{m}{M}\right)\left(\frac{760}{P}\right)\left(\frac{T}{300}\right)$$

where m = molar gas volume

M = molecular weight of ethylene glycol

F = carrier flow rate in mℓ/min

A manifold that could be used to prepare various concentrations of ethylene glycol is shown in Fig. 7. This is a simplified version of the one used by Hrubesh et al. to calibrate a formaldehyde monitor (Ref. 12). For high concentrations (> 1 ppm), they flowed the air over the heated permeation tube at whatever flow rate gave the desired concentration, then directly to the membrane separator. For lower concentrations, they obtained a fixed concentration of formaldehyde in air by an appropriate flow rate, then diluted the stream by pure air to the desired concentration.

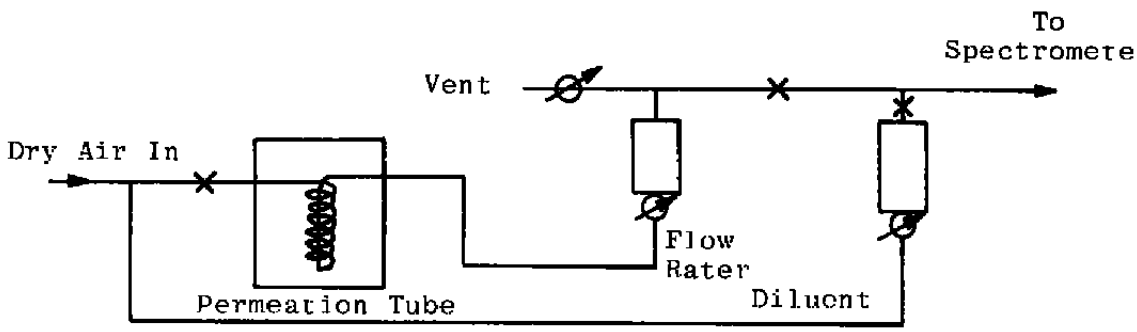

Figure 7. Calibration manifold.

To calibrate the spectrometer, the instrument should first be flushed with pure dry air for a couple of hours, and the chart recorder, voltmeter, or whatever instrument is used to record the output is zeroed. Then a known concentration of ethylene glycol is introduced into the instrument and time allowed for it to reach its full response. The response and the time to reach full response should be noted, and then continue flushing with pure air, noting

the decay time of the system. The procedure should be repeated with a different concentration but with the flow rate the same as before, and the sample concentration changed incrementally until the desired calibration range is obtained.

Other parameters that can be varied during these tests are the pressure in the cell and the microwave power. The conditions which give the most linear response up to high concentrations may not be the same as those that give the most sensitive response at low concentrations. The response time and decay time of the signal after switching back to a pure-air purge will indicate the extent of absorption onto the cell and inlet tubing walls. This memory, or hysteresis problem has been the Achilles heel for microwave spectrometers designed for the continuous monitoring of trace pollutants in the air. But a long lag in returning to the baseline after calibration would not be a problem for the application envisioned here.

4.4 RESONANT-CAVITY SPECTROMETER

A method that is largely self-calibrating is described in this section. A resonant cavity is essentially a hollow space enclosed by metallic walls that at resonance provides an extremely long path length through multiple reflections, and can store a considerable amount of microwave energy. A resonant cavity has several advantages as an absorption cell for microwave spectrometry. First, the sensitivity of a spectrometer is proportional to the effective path length of the radiation through the sample. The effective path length of a resonant cavity is given by (Ref. 14)

$$\ell_{eff} = \frac{\lambda^2}{\pi\lambda_g} Q_L \tag{60}$$

where λ is the wavelength of the radiation in free space, λ_g its wavelength in a waveguide, and Q_L the loaded Q of the cavity. The Q of the resonant cavity is given by ν_o/ν, the resonant frequency divided by the half-width of the Lorentzian mode shape. For the cavity to be proposed here, the Q will be about 20,000 giving an effective path length of about 10 m. A second advantage is that the resonator has a small volume, which is important for a portable instrument. Third, a resonant cavity has a small surface area. This is important in minimizing wall adsorption effects. Fourth, it is easy to saturate a molecular transition in a cavity because of the large power density within it. This property is desirable for the optimum power saturation method, which leads to linear response with concentration.

The cavity proposed here is of the semiconfocal type, in which a movable spherical mirror is aligned with a plane mirror (Fig. 8). This is preferred over two-plane reflectors because it minimizes diffraction losses, and the alignment of the mirrors is not as critical. The cavity is a transmission type, so that only power of the resonant frequency of the cavity will appear at the output. The first of the two reflectors is a planar surface through which is

passed two sections of millimeter waveguide to couple power into and out of the cavity. The second reflector is a concave spherical mirror of radius of curvature r mounted so that its separation from the plane mirror d is about r/2.

Figure 8. Semiconfocal resonant cavity.

Resonance conditions for microwave radiation of wavelength λ can be stated in terms of radius of curvature r and mirror spacing d as

$$\frac{4d}{\lambda} = 2q + (1 + m + n)\left\{1 - \frac{4}{\pi}\left[\tan^{-1}\left(\frac{r - 2d}{4 + 2d}\right)\right]\right\} \tag{61}$$

Here m, n, and q are the indices of the particular mode of resonance, i.e. TME_{mnq}, where

m = number of field reversals in a direction perpendicular to the axis of the cavity;

n = number of field reversals in a direction perpendicular to the axis of the cavity and to the m axis; and

q = number of integral half-wavelengths between the reflectors.

The fundamental resonant mode, the TEM_{ooq}, is the mode confined to the smallest cross-sectional area of the cavity; as the mirror radius a is reduced, radiation in this mode will suffer an increasing loss of power because of diffraction. It is usually desirable to support only the fundamental TEM_{ooq} mode, which can be done by adjusting the cavity dimensions so as to match the diffraction loss of the fundamental mode with coupling and conduction losses. A simple rule of thumb to accomplish this is to design the cavity to conform to the specifications (W. C. Oelfke, unpublished dissertation, Duke University, 1969)

$$a^2/r\lambda = 1 \tag{62}$$

where a is the radii of the mirrors. More detailed information on the performance of confocal resonant cavities may be found in the article by Boyd and Gordon (Ref. 15).

For radiation whose wavelength is only 3 or 4 mm, an effective path length on the order of 1 m may be achieved with a very small cavity. One of sufficient size would only need a

mirror radius of about 3 cm and a radius of curvature r for the spherical mirror of about 10 cm, so that the separation of the mirrors would be about 5 cm. Absorption of ethylene glycol would probably be minimized by gold plating the mirrors, which should be machined from Invar metal to reduce thermal variations in the cavity structure. The reflectors may be separated by a quartz spacer, and the vacuum seal achieved by Viton O-rings between the spacer and each plate. Viton O-rings are less adsorbant than the usual neoprene O-rings.

The transition from waveguide to cavity creates an impedance mismatch which will cause some of the microwaves to be reflected back to the Gunn effect diode. The Gunn diode will run quieter if an isolater is placed in the waveguide to shield it from reflections. The Gunn diode will not remain tuned to the absorption frequency if it is left free running. The usual method of stabilizing the microwave frequency is to use an oven-controlled low-frequency oscillator as a reference. The basic stability of the crystal oscillator can then be transferred to the microwave oscillator by multiplications and phase locking. The electronics attendant to phase-lock stabilization constitute the largest expense in a spectrometer with a solid-state source. The stabilizer can be a hindrance in a portable spectrometer and adds considerable weight and size to the instruments. Another drawback is that the crystal oscillator is very sensitive to vibrations.

Morrison and coworkers at the Lawrence Livermore Laboratory have developed a means of locking a source to an absorption line of the compound of interest (Ref. 8). The power from the source is split, with some of it sent to a cell containing a known concentration of ethylene glycol. This cell need be only a short length of waveguide. If a small amount of frequency modulation is applied to the microwave source, and if a detector that is sensitive to amplitude variations is used, a signal is obtained from the detector that is proportional to the slope of the gas absorption line. If that signal is applied to a phase-sensitive detector, the output signal is the derivative of the absorption line, which can be used to lock the source to the line.

In principle this scheme would work by itself, but it is possible for the microwave source to lock to extraneous absorptions that occur because of mismatches in the hardware. This problem may be overcome by the application of Stark modulation to the absorption cell and the use of a second phase-sensitive detector tuned to the frequency and phase of the Stark modulation (Fig. 9).

The resonant frequency of the cavity also needs to be locked to the center frequency of the absorption line. The cavity is slightly tunable because each O-ring will allow a plate movement of about ± 10 mm after a vacuum has been established in the cavity, while still maintaining the vacuum seal. For 90-GHz radiation, this allows the resonant frequency of the cavity to be varied by about 700 MHz. The tuning may be accomplished by the controlled thermal expansion of an aluminum spacer separating the two plates.

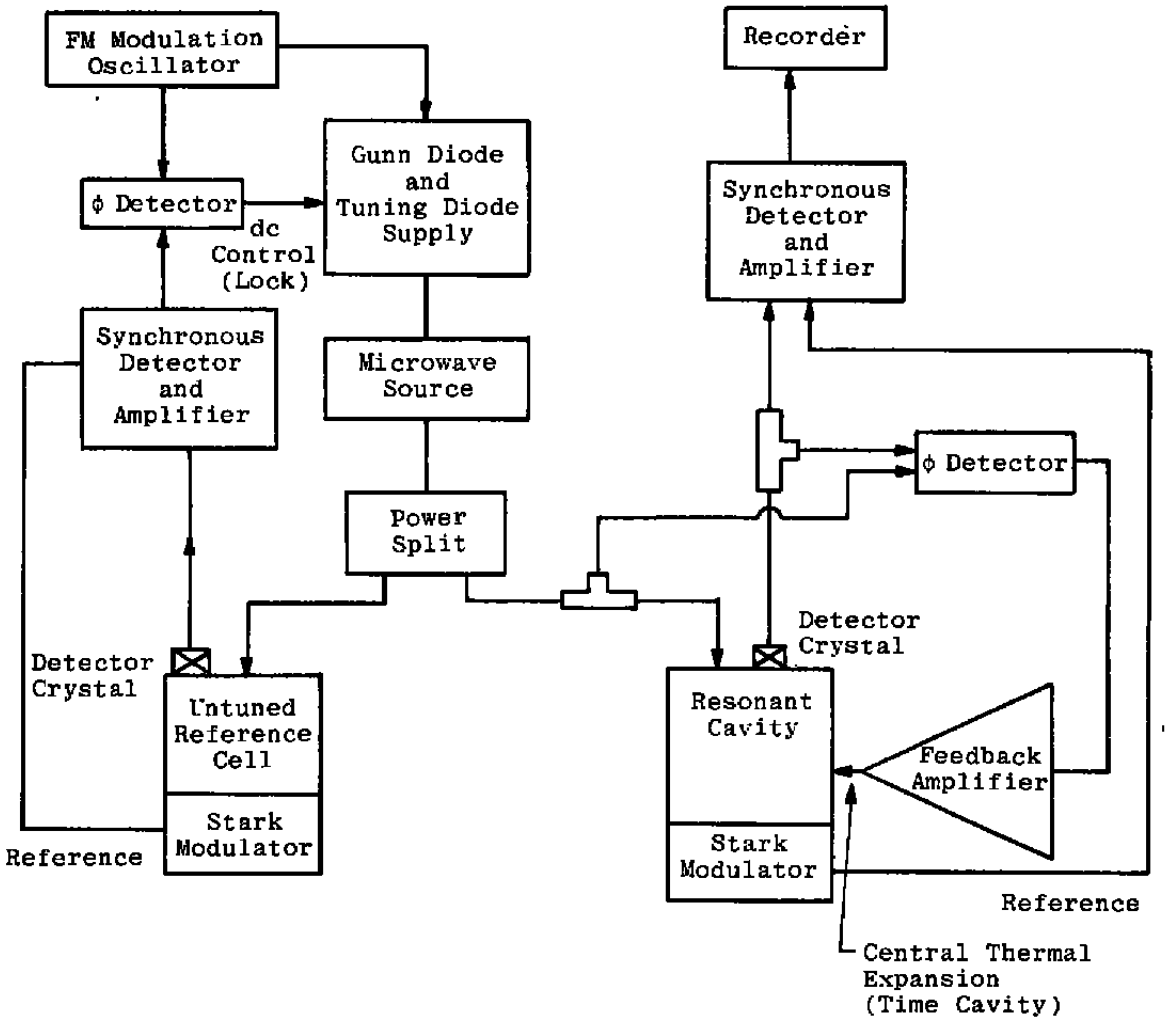

Figure 9. Resonant cavity spectrometer.

Once stable oscillations of the source are obtained at the desired frequency, it is possible to transfer this stability directly to the resonant frequency of the cavity. The cavity resonant frequency may be tuned by physically moving the two reflectors apart by the thermal expansion of the aluminum collar. As the cavity resonance approaches the source frequency, more microwave power will pass through the cavity to the detector. Part of the signal from the detector may be compared with a sample of the power directly from the source. As the cavity resonance approaches the microwave frequency, the microwaves at the output of the cavity have a positive phase angle compared to that of the input signal. Near resonance, the phase shift is a maximum of 90 deg positive and changes with a very sharp slope to another maximum of 90 deg positive and changes with a very sharp slope to another maximum of 90 deg negative, passing through zero-phase shift exactly when the cavity resonance matches the input frequency. If the input and output signals are compared by a phase detector, the dc

output from the phase detector may be amplified and used to control the current used to heat the aluminum collar. The cavity resonance is thus forced by this feedback loop to stay at the resonant frequency of the absorption line.

For very small quantities of absorbing gas in a mixture, the actual amount of microwave power absorbed is minute. As discussed earlier, the signal-to-noise ratio of a microwave spectrometer is greatly improved by the use of Stark modulation. Peak-to-peak field strengths as high as 2 kv/cm may be required to fully modulate absorption lines that are pressure broadened. Problems with gas breakdown and glow discharge within the cavity can arise with these high fields at the operating pressures. This could be alleviated by reducing the electrode spacing, but in the cavity, the two reflectors are used as electrodes and a reduction in spacing will lead to a reduction in cavity quality factor. A discharge within the cavity can damage the reflectors and lead to a reduction in quality factor.

A zero-based square wave at a frequency such as 10 kHz may be produced by a Stark modulator circuit with a peak-to-peak voltage as high as 3 kv (Appendix D). This voltage is applied to one reflector plate of the cavity so that the electric field appears through the sample. If ethylene glycol molecules are present in the cavity, the effect of this on-off field is to amplitude modulate the microwaves at a 10-kHz rate. Microwave frequency can be demodulated by a video detector crystal diode, leaving just the 10-kHz signal, which can be amplified and then phase compared with a reference signal derived directly from the Stark modulator circuit. The output of the phase detector is a dc signal that is proportional to the amplitude of the 10-kHz signal. This signal can then be further amplified, and an RC time constant applied to it before it is recorded.

Special care is required with the Stark modulator to prevent leakage of its signal and subsequent pickup by the detection electronics. Any such leakage could not be distinguished from the desired signal since they occur at the same frequency and phase. The modulator should be shielded by metal and placed as close to the resonant cavity as possible.

In order to minimize this problem, A. Maddox of the Lawrence Livermore Laboratory designed a small solid-state square-wave generator based on self-oscillating ferrite transformer (Ref. 8). It requires only a 24 vdc input, yet generates a square wave up to 3 kv peak-to-peak. It can be put on a printed circuit board and placed in an aluminum can that is mounted directly on the cavity itself.

The theoretical limit on the sensitivity for the detection of a rotational line in a resonant cavity whose loaded quality factor is Q_L can be calculated from the following equation (Ref. 16):

$$\alpha_{min} = \left(\frac{4k\,TN\Delta f}{P_{in}}\right)^{1/2} \frac{2\pi}{Q_L \lambda} \tag{63}$$

where α_{min} = the minimum detectable absorption coefficient for the system;

k = Boltzmann's constant;

T = absolute temperature;

N = noise figure for the system;

Δ_f = detection bandwidth;

P_{in} = microwave power in; and

λ = the wavelength of the radiation.

Reasonable values for these parameters are $N = 30$, $\Delta_f = 0.01$ Hz, $P_{in} = 10^{-4}$ W, and $Q_L = 10{,}000$. With $T = 300$ K and $\lambda = 0/.3$ cm, we get $\alpha_{min} \approx 6 \times 10^{-11}$ cm^{-1}. If the maximum absorption coefficient of the absorption line is 6×10^{-5}, the theoretical limit of detectability, given by the ratio of these two quantities, is found to be about 1.0 ppm. In practice one would not expect such good sensitivity, but with a membrane separator, it should be possible to detect concentrations even smaller than this. The highest sensitivity will occur when a long RC time constant (e.g., one minute) is employed.

The spectrometer can directly give quantitative information if its output can be made to respond linearly to the total amount of absorption by the ethylene glycol molecules. A necessary condition for linear response to the peak of an absorption line is that the width of the observed transition must remain constant (Ref. 8). This will be nearly true when the absorbing gas occurs in trace quantities in a mixture of other gases, such as air, since the linewidth will then be determined mainly by collisions with N_2 and O_2 molecules, whose concentration remains constant. This linear response will be upset if there are variations in the amount of water vapor because polar molecules like water have a much greater line-broadening effect than do nonpolar molecules like N_2 and O_2. The dimethyl silicone membrane will increase the water vapor concentration of the sample by a factor as high as 100. If the amount of water vapor varies significantly from one run to the next, the sample will need to be dried before it is passed through the cavity. A material would need to be found that dries the sample while removing only a small part of the ethylene glycol. Phosphorous pentoxide is a likely candidate for such a material.

The optimum power saturation method as described by Harrington (Ref. 17) will give a linear response for a given line independent of the line width. This method works well with a cavity spectrometer because the saturation conditions are so easy to meet. The line width will remain nearly constant if the sample remains fairly dry and if the operating pressure is kept constant. Since relaxation back to the ground state is brought about mainly by collisions with N_2 molecules, the power needed to saturate the line is independent of the amount of ethylene glycol present. To employ the optimum power method, the level of microwave power into the absorption cell should be sufficient to just begin to saturate the line. The optimum power for a given gas and spectrometer must be determined experimentally, but for the situation described here, it is probably on the order of 100 μw. The power sent to the cavity may be controlled by means of a variable attenuator.

The optimum pressure in the cell must also be determined experimentally. The strength of the signal will increase as the sample pressure increases up to the point where the Stark field is not sufficient to fully modulate the absorption line. The optimum operating pressure would probably be in the range of tens of millitor. A list of components for the cavity spectrometer is found in Appendix C.

5.0 CONCLUSION

A study has been conducted to determine if microwave spectroscopy techniques could be used to detect small concentrations of ethylene glycol in airstreams. The study consists of a close look at the theory of microwave spectroscopy, as well as a summary of what is known about the spectra of the ethylene glycol molecule. With this background, three different microwave spectrometer designs are proposed, each of which should be capable of making the required measurements.

First, a fast-scan, low-resolution microwave spectrometer to operate near 17.1 GHz is described. There are many ethylene glycol absorption lines around 17.1 GHz. If a microwave spectrometer were used to scan a range centered about 17.1 GHz, a distinct spectrum would be obtained whenever ethylene glycol was present. This spectrometer could be operated at a pressure as high as 0.5 torr without loss of sensitivity because of pressure broadening. The absorption cell would be a length of waveguide, and a fully automated microwave source can be purchased. The sensitivity can be increased by the use of permselective membranes to enrich the concentration of ethylene glycol in the air mixture. The airstream being sampled should be predried, as water vapor increases the pressure broadening of absorption lines. The pumping lines should be kept as short as possible on all systems, as ethylene glycol may condense on the surface of the pumping lines and the absorption cell walls. The effect of this condensation is to cause the system to have a long response time. This system should be applicable to concentrations greater than 10 to 20 ppm.

Second, a simple microwave spectrometer to detect ethylene glycol could be constructed using a solid-state source of monochromatic microwave power. Using a solid-state source such as a Gunn effect diode, the entire source package including the power supply would be small and lightweight. The simplest design would use the Gunn diode as both the oscillator and detector. The output could be tuned with a varacter tuning diode positioned side-by-side with the Gunn diode in the waveguide cell. A spectrometer of this type operating in the 80-to 90-GHz range should be capable of detecting concentrations of ethylene glycol as low as 5-to 10 ppm.

The third design, a resonant cavity microwave spectrometer, has several advantages over the other microwave spectrometers. The sensitivity of a spectrometer is proportional to the effective path length of the radiation through the sample. The cavity can be designed to give a long, effective path length while keeping the actual volume small. The small volume is important for designing a portable instrument, but an even more important consideration is that a small cavity has a small surface area which minimizes wall absorption effects. Also, it is easy to saturate a molecular transition in a cavity because of the large power density within the cavity. A disadvantage is that the Gunn diode will not remain tuned to the absorption frequency unless some method is used to stabilize the microwave frequency. The amount of microwave power absorbed is quite small and Stark modulation is needed to improve the signal-to-noise ratio. The spectrometer can give quantitative information directly if its output responds linearly to the total absorption by the ethylene glycol molecules. A necessary condition for linear response is that the width of the transition remain constant. The line width will remain nearly constant if the sample remains dry, and the operating pressure is kept constant. This instrument should be sensitive to concentrations less than 1 ppm.

In conclusion, microwave spectroscopy does provide a way of detecting ethylene glycol in airstreams. It would provide a sensitivity of at least 10 ppm, and possibly greater sensitivity can be achieved if necessary.

REFERENCES

1. Merzbacher, Eugen. *Quantum Mechanics.* John Wiley & Sons, New York, 1970.

2. Gordy, W. and Cook, R. L. *Microwave Molecular Spectra.* John Wiley & Sons, New York, 1970.

3. Wacker, P. F. and Pratto, M. R. *Microwave Spectral Tables. Line Strengths for Rotational Transitions for Asymmetric Rotor Molecules*, Vol. II, Pergamon Press, London.

4. Walder, E., Bauder, A., and Gunthard, H. *Chemical Physics*, Vol. 51, 1980, p. 223.

5. Caminati, W. and Corbelli, G. *Journal of Molecular Spectroscopy*, Vol. 90, 1981, p. 572.

6. Buckley, P. and Giguere, P. A. *Canadian Journal of Chemistry*, Vol. 45, 1967, p. 397.

7. Hughes, R. H. and Wilson, E. G., Jr. *Physical Review*, Vol. 71, 1947, p. 562.

8. Morrison, R. L., Maddux, A. and Hrubesh, L., Lawrence Livermore Laboratory Report UCRL-51945, 1975.

9. Lazarus, M. J., Novak, S. and Bullimore, E. D. *Microwave Journal*, Vol. 14, 1971, p. 43.

10. Hrubesh, L. W. and Varma, C. *Chemical Applications of Microwave Rotational Spectroscopy*, Addison-Wesley, New York, 1977.

11. Marstokk, K. M. and Mollendal, H. *Journal of Molecular Structure*, Vol. 22, 1974, p. 301.

12. Hrubesh, L. W. et al. Lawrence Livermore Laboratory Report UCID-16488, 1974.

13. Metronics Associates, Inc., Tech. Bulletin No. 7-70, Dynacal Permeation Tubes.

14. Gordy, W., Smith, W. V. and Trambarulo, R. F. *Microwave Spectroscopy*, John Wiley & Sons, New York, 1953.

15. Boyd, G. D. and Gordon, J. P. "Confocal Multimode Resonator for Millimeter Optical Wavelength Masers." Vol. No. 2, March 1961, pp. 489–508.

16. Townes, C. H. and Schawlow, A. L. *Microwave Spectroscopy*, McGraw-Hill, New York, 1955.

17. Harrington, H. W. "On the Separation of the Broadening-Relaxation Time and Molecular Concentration from Pure-Rotational Spectroscopic Intensity Data." *Journal of Chemical Physics*, Vol. 46, No. 10, May 15, 1967, pp. 3698–3707.

APPENDIX A
MICROWAVE SPECTRUM OF ETHYLENE GLYCOL

The following table gives the frequency of the ethylene glycol absorption lines in the 8- to 38-GHz region. Frequencies are accurate to within ± 0.10 MHz in the 12.4- to 38-GHz region and to within ± 2 MHz in the 8- to 12.4-GHz region.

Frequency, MHz				
8198	8222	8283	8328	8353
8461	8529	8668	8756	8762
8794	8815	8882	8957	9031
9113	9197	9322	9380	9514
9587	9827	9875	9907	9992
10130	10319	10418	10533	10625
10675	10711	10741	10815	10913
10952	10989	11024	11060	11103
11190	11352	11484	11540	11727
11748	11762	11786	11837	12158
12371	12436.97	12440.30	12449.29	12493.03
12503.08	12599.89	12625.63	12688.60	12775.38
12863.86	12872.32	12928.52	12972.95	12992.82
13018.77	13037.21	13051.86	13056.63	13060.77
13076.18	13155.08	13212.85	13231.08	13264.38
13284.32	13351.47	13370.95	13395.61	13488.89
13492.80	13593.72	13618.26	13687.75	13758.00
13769.56	13777.38	13828.04	13832.70	13930.31
13934.60	14015.93	14023.82	14076.63	14081.23

Frequency, MHz				
14090.84	14130.28	14185.45	14196.13	14286.77
14288.88	14412.40	14420.85	14434.36	14435.81
14453.69	14523.02	14524.63	14531.75	14545.50
14548.40	14549.78	14585.61	14605.11	14612.38
14615.81	14653.89	14663.57	14716.30	14758.28
14806.13	14870.30	14962.43	14981.15	14983.60
14986.94	14990.52	15003.56	15124.53	15195.97
15206.22	15214.11	15286.10	15320.49	15344.38
15347.75	15366.53	15375.75	15382.67	15397.69
15425.06	15438.66	15474.10	15484.23	15528.75
15536.76	15563.92	15582.85	15623.23	15624.00
15632.92	15639.69	15643.95	15660.32	15667.97
15686.36	15702.89	15714.10	15741.41	15786.11
15796.74	15811.03	15816.77	15827.41	15836.56
15857.97	15865.41	15867.03	15878.92	15906.75
15953.06	15958.05	15985.75	16005.39	16020.07
16043.17	16054.33	16094.22	16103.69	16106.09
16142.97	16176.34	16206.52	16223.93	16253.35
16295.96	16305.75	16322.66	16340.59	16341.52
16357.65	16364.93	16439.03	16444.48	16446.48

Frequency, MHz				
16458.67	16501.16	16505.90	16513.21	16533.74
16541.05	16570.12	16588.11	16615.51	16620.30
16625.36	16633.62	16647.97	16655.18	16660.75
16665.16	16675.52	16683.66	16687.70	16716.48
16719.42	16726.71	16732.21	16735.06	16764.20
16772.20	16789.60	16794.43	16800.15	16803.95
16814.52	16820.27	16838.82	16841.33	16847.21
16859.82	16868.96	16887.93	16894.52	16899.5
16907.33	16914.85	16923.52	16928.26	16943.64
16945.80	16946.83	16978.41	16987.80	16988.96
17013.10	17020.19	17023.23	17025.81	17045.16
17048.30	17064.21	17077.73	17084.22	17085.23
17108.58	17109.64	17111.33	17115.47	17122.03
17127.60	17129.48	17138.57	17144.38	17156.60
17165.19	17174.68	17187.30	17195.96	17205.05
17205.86	17215.49	17226.12	17228.00	17236.13
17259.42	17268.35	17285.96	17296.88	17301.30
17307.80	17317.63	17335.87	17337.70	17340.78
17346.91	17347.40	17370.92	17382.98	17402.53
17414.00	17472.80	17473.52	17479.87	17497.90

Frequency, MHz				
17512.23	17514.41	17533.22	17579.20	17601.73
17619.63	17628.75	17634.16	17643.53	17657.30
17679.25	17699.76	17713.57	17724.15	17737.86
17753.00	17759.97	17779.04	17791.39	17797.18
17828.80	17839.99	17872.29	17893.63	17927.66
17929.62	17937.59	17949.00	17958.83	17989.31
17994.24	18002.27	18011.77	18016.35	18020.07
18139.82	18147.16	18153.96	18190.55	18197.88
18218.71	18246.58	18251.85	18300.18	18306.43
18329.78	18357.05	18372.29	18418.11	18422.34
18436.99	18452.81	18539.55	18554.44	18581.17
18591.80	18599.85	18609.86	18645.65	18650.67
18724.59	18764.73	18793.85	18812.88	18850.12
18852.50	18858.55	18859.74	18940.24	18962.23
18970.20	18981.75	18998.54	19025.07	19060.60
19065.14	19079.11	19086.12	19097.38	19106.39
19136.19	19138.67	19210.48	19239.63	19245.59
19262.06	19275.06	19292.03	19298.5	19342.37
19449.44	19451.15	19493.93	19567.21	19575.85
19584.32	19614.58	19628.44	19669.41	19732.19

Frequency, MHz				
19781.42	19798.14	19843.65	19853.82	19859.50
19873.3	19929.62	19984.42	20016.17	20117.78
20177.43	20355.40	20359.98	20376.68	20383.56
20587.47	20683.57	20713.49	20813.50	20842.71
20878.56	20964.85	20998.6	21015.22	21020.63
21099.95	21169.91	21237.96	21259.57	21260.95
21268.32	21269.40	21280.93	21285.44	21298.05
21341.59	21347.22	21441.59	21551.90	21552.93
21580.27	21715.43	21785.01	21786.16	21802.60
21844.85	21894.65	21945.84	21969.32	21976.56
21981.07	21983.08	21994.88	22015.48	22039.16
22072.54	22075.24	22088.82	22115.35	22119.33
22148.16	22183.87	22196.95	22202.39	22219.45
22240.72	22306.17	22307.73	22452.61	22457.10
22575.13	22697.25	22733.84	22758.72	22792.39
23078.53	23312.57	23381.28	23393.88	23389.43
23472.91	23504.54	23507.85	23554.43	23555.66
23566.00	23624.46	23637.68	23687.07	23693.25
23697.30	23713.49	23720.14	23753.04	23761.87
23773.76	23811.78	23818.33	23872.96	23911.55

Frequency, MHz				
23922.9	23987.05	23989.84	23990.54	24007.50
24015.65	24018.23	24027.97	24032.68	24034.22
24046.93	24065.80	24101.50	24121.76	24130.08
24167.86	24237.44	24243.03	24324.53	24366.10
24377.80	24411.10	24488.44	24501.20	24512.23
24612.40	24615.29	24670.90	24687.32	24737.44
24779.03	24829.54	24863.05	24882.49	24885.80
24930.40	24986.96	24988.29	25003.63	25009.44
25019.21	25027.70	25031.37	25040.23	25044.12
25105.88	25111.40	25113.59	25129.75	25237.36
25298.8	25359.93	25452.54	25467.95	25522.55
25529.99	25532.87	25576.48	25580.58	25604.39
25615.50	25636.58	25642.71	25754.41	25801.13
25816.08	25831.88	25845.86	25987.66	26015.70
26165.92	26190.84	26195.15	26281.06	26330.67
26332.91	26381.65	26488.72	26559.05	26572.56
26651.28	26810.86	26968.32	27122.24	27146.13
27268.45	27400.11	27421.44	27564.66	27727.05
27796.17	27934.39	28044.59	28178.64	28194.66
28351.89	28501.50	28648.11	28915.68	29060.21
29134.32	29190.96	29203.51	29238.22	29261.43
29345.46	29377.13	29485.93	29515.26	29522.52

Frequency, MHz				
29623.86	29762.80	29896.99	29982.26	30030.08
30116.71	30435.08	30464.59	30593.78	30683.82
30689.66	30730.32	30787.13	30885.56	30985.52
31044.40	31086.00	31187.43	31288.62	31390.04
31491.74	31565.17	31575.84	31593.18	31612.80
31695.68	31732.11	31737.05	32068.27	32248.10
32378.09	33174.02	33186.31	33200.12	33207.24
33228.03	33232.85	33239.62	33260.72	33272.94
33293.92	33308.63	33313.47	33331.04	33371.13
33437.30	33482.41	33581.18	33588.95	33598.64
33631.15	33639.96	33674.21	33702.24	33798.67
33803.38	33806.40	33816.97	33826.81	33907.60
33977.01	33994.64	34222.56	34465.50	34749.80
34873.71	34948.82	35064.90	35138.94	35268.28
35269.50	35298.24	35347.47	35411.09	35482.00
35564.81	35609.04	35658.52	35673.96	35764.61
35884.37	35951.08	35987.91	35995.59	36018.08
36030.51	36061.57	36079.54	36084.83	36157.32
36166.70	36424.85	36525.01	36525.78	36993.07
37175.23	37187.78	37362.02	37392.94	37443.23
37495.36	37557.36	37636.14	37696.72	37714.37
37739.48	37741.70	37780.49	37790.09	37830.78
38800.35				

APPENDIX B
VIBRATIONAL FREQUENCIES OF ETHYLENE GLYCOL (REF. 16)

Mode	Frequency (cm^{-1})
O-H stretch	$\nu_1 = \nu_{14} = 3660$
CH stretch symmetrical	$\nu_2 = \nu_{15} = 2940$
CH stretch antisymmetrical	$\nu_3 = \nu_{16} = 2880$
CH_2 scissor	$\nu_4 = \nu_{17} = 1456$
CH_2 wag	$\nu_5 = \nu_{18} = 1385$
COH bend	$\nu_6 = 1160$ $\nu_{19} = 1160$
CH_2 twist	$\nu_7 = 1279$ $\nu_{20} = 1254$
C-O stretch	$\nu_9 = \nu_{18} = 1036$
CH_2 rocking	$\nu_{10} = \nu_{22} = 868$
C-O torsion	$\nu_{12} = \nu_{24} = 375$
CCO bend	$\nu_{11} = \nu_{23} = 522$
C-C torsion	$\nu_{13} = 220$

APPENDIX C
PARTS LISTS FOR PROPOSED SPECTROMETER DESIGNS

A. 17-GHz Stark Modulation Spectrometer

Microwave source
Attenutator
Waveguide cell
Flanges
Vacuum pump and air pump
Two-vacuum windows
Separator
Detector
Stark modulator
Lock-in amplifier
Recorder
Cables and miscellaneous hardware (fittings, tubing, valves)

B. Simple Gunn Effect Diode Spectrometer

Gunn effect diode
Varactor tuning diode
Power supplies
Attenuator
Two-vacuum windows
Cell
Separator
Vacuum pump and air pump
Modulator and Synchronous detector
Recorder

C. Resonant-Cavity Spectrometer

Gunn effect diode
Varactor tuning diode
Power supplies
Power splitter
Two-directional couplers
Untuned reference cell

Resonant cavity
Waveguide isolator
Two Stark modulators
Separator
Two Detectors
Two Synchonous detector
Two-Phase detector
Modulation oscillator
Feedback amplifier
Vacuum pump and air pump
Four Vacuum windows
Recorder
Miscellaneous hardware (fittings, tubing, valves)

APPENDIX D
COMPACT 10-kHz STARK MODULATOR